Food and Chemical Toxicology 123 (2019) 125–141

Contents lists available at ScienceDirect

Food and Chemical Toxicology

journal homepage: www.elsevier.com/locate/foodchemtox

5-HT_{1A} receptor agonist 8-OH-DPAT induces serotonergic behaviors in mice via interaction between PKCδ and p47phox

Hai-Quyen Tran[a,1], Eun-Joo Shin[a,1], Bao-Chau Hoai Nguyen[a], Dieu-Hien Phan[a], Min-Ji Kang[a], Choon-Gon Jang[b], Ji Hoon Jeong[c], Seung-Yeol Nah[d], Akihiro Mouri[e], Kuniaki Saito[e], Toshitaka Nabeshima[e,f,g], Hyoung-Chun Kim[a,*]

[a] Neuropsychopharmacology and Toxicology Program, College of Pharmacy, Kangwon National University, Chunchon, 24341, Republic of Korea
[b] Department of Pharmacology, School of Pharmacy, Sungkyunkwan University, Suwon, 16419, Republic of Korea
[c] Department of Pharmacology, College of Medicine, Chung-Ang University, Seoul, 06974, Republic of Korea
[d] Ginsentology Research Laboratory and Department of Physiology, College of Veterinary Medicine, Konkuk University, Seoul, 05029, Republic of Korea
[e] Advanced Diagnostic System Research Laboratory, Fujita Health University Graduate School of Health Science, Aichi, 470-1192, Japan
[f] Aino University, Ibaraki, 576-0012, Japan
[g] Japanese Drug Organization of Appropriate and Research, Nagoya, 468-0069, Japan

ARTICLE INFO

Keywords:
Serotonergic behaviors
5-HT_{1A} receptor
PKCδ knockout mice
p47phox knockout mice
Interaction between 5HT_{1A} receptor
PKCδ, and p47phox
Hypothalamus

ABSTRACT

Serotonin syndrome is an adverse reaction due to increased serotonin (5-hydroxytryptophan: 5-HT) concentrations in the central nervous system (CNS). The full 5-HT_{1A} receptor (5-HT_{1A}R) agonist (±)-8-hydroxy-dipropylaminotetralin (8-OH-DPAT) has been recognized to elicit traditional serotonergic behaviors. Treatment with 8-OH-DPAT selectively increased PKCδ expression out of PKC isoforms and 5-HT turnover rate in the hypothalamus of wild-type mice. Treatment with 8-OH-DPAT resulted in oxidative burdens, co-immunoprecipitation of 5-HT_{1A}R and PKCδ, and phosphorylation and membrane translocation of p47phox. Importantly, p47phox also interacted with 5-HT_{1A}R or PKCδ in the presence of 8-OH-DPAT. Consistently, the interaction and oxidative burdens were attenuated by 5-HT_{1A}R antagonism (i.e., WAY100635), PKCδ inhibition (i.e., rottlerin and genetic depletion of PKCδ), or NADPH oxidase/p47phox inhibition (i.e., apocynin and genetic depletion of p47phox). However, WAY100635, apocynin, or rottlerin did not exhibit any additive effects against the protective effect by inhibition of PKCδ or p47phox. Furthermore, apocynin, rottlerin, or WAY100635 also significantly protected from pro-inflammatory/pro-apoptotic changes induced by 8-OH-DPAT. Therefore, we suggest that 8-OH-DPAT-induced serotonergic behaviors requires oxidative stress, pro-inflammatory, and pro-apoptotic changes, that PKCδ or p47phox mediates the serotonergic behaviors induced by 8-OH-DPAT, and that the inhibition of PKCδ-dependent p47phox activation is critical for protecting against serotonergic behaviors.

1. Introduction

Serotonin syndrome, or serotonin toxicity, is a serious disorder attributable to exaggerated serotonergic function in the brain, most commonly after antidepressant overdose or after combining several psychotropic medications (Boyer and Shannon, 2005). It has been suggested that the serotonin syndrome has become an increasingly common clinical problem, reflecting the rising use of drugs that enhance serotonergic transmission (Graudins et al., 1998; Isbister et al., 2004; Thanacoody, 2012). Serotonergic behaviors can be induced by the excess of serotonin (5-hydroxytryptophan: 5-HT) precursor or receptor agonists, increased release of 5-HT, and reduced 5-HT reuptake or metabolism (Bijl, 2004; Birmes et al., 2003; Gillman, 2004; Kalueff et al., 2008).

It has been currently elusive whether the serotonin syndrome induces overall 5-HT receptor (5-HTR) activation or whether it can be attributable to stimulation of the specific 5-HTR. Serotonergic behaviors, such as backward walking, flat body posture, forepaw treading, head weaving, hind-limb abduction, Straub tail, and tremor, as well as the autonomous response hypothermia have been demonstrated following administration of 5-HT_{1A}R agonist (Bert et al., 2006; Blanchard et al., 1997; Fox et al., 2007; Yamada et al., 1988). In particular, the full 5-HT_{1A}R agonist (±)-8-hydroxy-dipropylaminotetralin (8-OH-DPAT) has been demonstrated to elicit “traditional serotonin syndrome

* Corresponding author.
E-mail address: kimhc@kangwon.ac.kr (H.-C. Kim).
[1] First two authors (HQ Tran and EJ Shin) equally contributed to this work.

https://doi.org/10.1016/j.fct.2018.10.049
Received 5 July 2018; Received in revised form 18 October 2018; Accepted 22 October 2018
Available online 24 October 2018
0278-6915/

behaviors" (Fox et al., 2007; Haberzettl et al., 2013; Smith and Peroutka, 1986; Yamada et al., 1988).

The 5-HTRs are shown to activate several different protein kinases, such as serin-threonine, tyrosine, and lipid kinases (Raymond et al., 2001). Earlier reports suggested that 5-HT_{1A}R activates protein kinase C (PKC) (Liu and Albert, 1991; Middleton et al., 1990; Raymond et al., 2001, 1989). PKC family is a group of serine/threonine kinases, and it plays a key role in the regulation of diverse cellular functions, including proliferation, differentiation, proinflammation, and tumorigenesis (Giorgi et al., 2010). Recently, we have reported that the up-regulation of 5-HT_{1A}R induced by dextromethorphan facilitates the specific induction of PKCδ (Tran et al., 2018), indicating the potential role of PKCδ in the serotonergic behaviors mediated by 5-HT_{1A}R.

NADPH oxidase (PHOX) is a multi-unit enzyme complex responsible for the production of both extracellular and intracellular reactive oxygen species (ROS) by phagocytic cells. PHOX is comprised of cytoplasmic subunits (p47phox, p67phox, p40phox and Rac2), which upon phosphorylation by specific kinases, can form a complex and translocate to the membrane to dock with the membrane subunits (gp91, and p22phox) (Babior, 1999). It is well-recognized that p47phox acts as a connector between the components of the membrane and the cytoplasm (Reeves et al., 1999). PHOX emerged as a novel class of molecular targets for the treatment of neurodegenerative disorders due to its role of oxidant generation (Sorce et al., 2017). Moreover, we (Tran et al., 2018) and others (Mukhin et al., 2000) demonstrated that the activation of 5-HT_{1A}R facilitates oxidant generation. These reports prompted us to investigate whether oxidant generation is contributable to the activation of PHOX by the 5-HT_{1A}R.

In view of increasing clinical problems due to an introduction of novel serotonergic drugs, the incorporation of animal models of the serotonin syndrome into the preclinical evaluation phase of a drug's toxicity profile is helpful, and will be essential for risk assessment in the future. Toxic responses of the serotonin syndrome can only be experimentally evaluated in humans with caution, and evidence for toxic effects is generally based on case studies of the serotonin syndrome, which are inconsistently reported (Boyer and Shannon, 2005). However, animal studies do allow experimental examinations of serotonergic responses following administration of direct and indirect 5-HTR agonists, and can serve as a method to assess drugs suspected in cases of the serotonin syndrome in humans. Moreover, it is recognized that more and more atypical antipsychotics possess 5-HT_{1A}R agonist properties (Kaneda et al., 2001). Therefore, we selected 8-OH-DPAT in order to achieve a better understanding of the role of 5-HT_{1A}R in serotonin syndrome behaviors.

Because 8-OH-DPAT-induced 5-HT turnover rate was most pronounced in the hypothalamus among prefrontal cortex, hippocampus and hypothalamus (Supplementary Fig. S2), we have focused on the hypothalamus for the neurochemical study. In addition, we observed that 8-OH-DPAT selectively induces PKCδ. Thus, we investigated whether genetic inhibition of PKCδ or p47phox positively modulates 8-OH-DPAT-induced serotonin syndrome behaviors. We observed here for the first time that PKCδ-dependent p47phox activation (i.e., phosphorylation and membrane translocation), as well as interactive modulation between 5-HT_{1A}R and PKCδ/p47phox, are important for inducing 8-OH-DPAT-induced serotonergic behaviors in mice.

2. Experimental procedures

2.1. Animals

All animals were treated in strict accordance with the National Institutes of Health (NIH) Guide for the Humane Care and Use of Laboratory Animals (NIH Publication No. 85–23, 1985; www.dels.nas.edu/ila). The present study was performed in accordance with the Institute for Laboratory Research (ILAR) Guidelines for the Care and Use of Laboratory Animals. Mice were maintained on a 12:12 h light/dark cycle and fed ad libitum. The room temperature was kept constant. They were adapted for 2 weeks to the above conditions prior to the experiments.

Wild-type (WT) C57BL/6 and p47phox knockout (KO) mice were purchased from Jackson Laboratories (Bar harbor, Maine, U.S.A.) (Dang et al., 2018, 2016). The PKCδ KO mice have been previously described (Shin et al., 2016, 2014, 2012, 2011). A breeding pair of PKCδ (±) mice, originally bred into a C57BL/6/J background, was a gift from Dr. K. I. Nakayama (Deptment of Molecular Genetics, Medical Institute of Bioregulation, Kyushu University, Fukuoka, Japan) (Miyamoto et al., 2002). These mice were subsequently maintained and bred into the C57BL/6/J background for six generations in a specific pathogen-free (SPF) mice facility before use with WT mice from the same litter in our experiments. Tail DNA was evaluated to genotype WT and PKCδ KO mice. Polymerase chain reaction (PCR) primers for genotyping were as follows: 5′-GGAAGAATAAGAAACTGCAT CACC-3′ and 5′-GAAGGAGC CAGAACCGAAAG-3′ for endogenous detection, and 5′-GGAAGAATAA GAAA CTGCATCACC-3′ and 5′-TGGGGTGGGATTAGATAAAT G-3′ for mutant detection (Bioneer Corporation, Daejeon, Republic of Korea).

2.2. Drug treatment

(±)-8-Hydroxy-dipropylaminotetralin (8-OH-DPAT; Sigma–Aldrich, St. Louis, MO, USA) and WAY100635 (Sigma-Aldrich, St. Louis, MO, USA), a 5-HT_{1A}R antagonist, were dissolved in 0.9% sterile saline immediately prior to use. Rottlerin (Biomol Research Laboratories Inc., Plymouth, PA, U.S.A.), a PKCδ inhibitor, was dissolved in dimethyl sulfoxide (DMSO) as a stock solution and then stored at − 20 °C. Rottlerin was diluted in sterile saline immediately before use at a concentration of 1 μg/μL. Apocynin (Sigma-Aldrich, St. Louis, MO, USA) was dissolved in DMSO and then diluted in sterile saline immediately prior to use at a concentration of 50 mg/ml. The final DMSO concentration was 10% (v/v).

Male C57BL/6/J background wild-type (WT) mice, weighing approximately 23 ± 2 g, were treated with a single dose of 8-OH-DPAT (2 mg/kg, i.p.) or saline. The dose of 8-OH-DPAT was determined based on a previous study (Fox et al., 2007).

To clarify the role of PKCδ and p47phox in 8-OH-DPAT-induced serotonin syndrome-like behaviors, rottlerin (3 μg, i.c.v./brain) was given 6 h and 2 h before 8-OH-DPAT treatment, and apocynin (50 mg/kg, i.p.) or WAY100635 (1 mg/kg, i.p.) was given 30 min prior to 8-OH-DPAT administration. The doses of rottlerin and WAY100635 were determined based on our previous study (Tran et al., 2018). Administration of apocynin (50 mg/kg, i.p.) was conducted once daily for seven consecutive days. The last dose of apocynin was given 30 min before 8-OH-DPAT injection. The dose of apocynin was determined based on our previous study. It was reported that 8-OH-DPAT concentration rapidly peaks in brain at 15 min after the drug administration (Yu and Lewander, 1997). In addition, the serotonergic behavioral syndrome induced by 8-OH-DPAT occurred rapidly 5 min after the drug administration, and disappeared 30 min later (Yu and Lewander, 1997). Moreover, the hypothermic and biological responses were maximal 45–60 min post-8-OH-DPAT administration (Yu and Lewander, 1997). In addition, consistent results were observed that the most significant behavioral changes induced by 8-OH-DPAT occurred within a short time after the drug administration (Fox et al., 2007; Haberzettl et al., 2013, 2014). Therefore, mice were sacrificed 15 min, 30 min, 1 h, 2 h, 6 h, 12 h, and 24 h after the 8-OH-DPAT treatment in our study. To ensure preservation of the neurochemical environment, and to minimize degradation during tissue dissection, decapitation was rapidly conducted. For Western blot analysis and other neurochemical assay, the brains were quickly removed; the hypothalamic, hippocampal, and prefrontal cortical tissues from both hemispheres were collected, and the tissues were instantly frozen in liquid nitrogen and kept at − 70 °C within an estimated time of 30 s from sacrifice.

2.3. Serotonergic behaviors

On test days, mice were moved to the testing room in their home cage 2 h prior to testing to allow for habituation to the environment. All experiments were conducted between 10:00 and 13:00 in a sound attenuated chamber. For each 60 min trial, four mice were tested at the same time. Each mouse was placed in the center of a black painted cage (260 mm × 200 mm x 140 mm) immediately after drug or vehicle administration. Between each trial, the cages were cleaned with 70% ethanol and paper towels.

Serotonergic behaviors induced by 8-OH-DPAT (2 mg/kg, i.p.) were evaluated in male WT, p47phox KO, and PKCδ KO mice. In our study, 8-OH-DPAT was administered after 15 min of habituation in a large Plexiglass cylinder. Behavioral assessments were made based on previous methods (Fox et al., 2007; Izumi et al., 2006; Tran et al., 2018). Behaviors associated with the rodent serotonin syndrome were recorded for five 1-min periods starting 5 min after drug administration. In each assessment period, the following behaviors were recorded: intermittent behaviors including head weaving, forepaw treading and backward movement (scored on a scale of 0–4; 0 = absent, 1 = present once, 2 = present several times, 3 = present frequently, 4 = present continuously); continuous behaviors included hind limb abduction, Straub tail, tremor, and low body posture (scored on a scale of 0–4; 0 = absent, 1 = perceptible, 2 = weak, 3 = medium, 4 = maximal). The scores from the five 1-min periods were summed together for each behavior. Overall serotonergic behavior scores were calculated for each 5-min assessment (Fox et al., 2007; Jacobs, 1976; Tran et al., 2018). Assessments were performed by observers blind to the genotype of the mice.

2.4. Rectal temperature

Rectal temperature under ambient temperature (21 ± 1 °C), was measured by inserting a thermometer probe lubricated with oil at least 3 cm into mice rectums. To prevent sudden movements of mice treated with 8-OH-DPAT, they were gently handled with a wool glove while their tail was moved to allow probe insertion. This was done to reduce any effect of restraint stress on rectal temperature. When the attempt to insert the probe was not successful (i.e., sudden movements of the animal or the need to restrain the mouse), the animal was excluded from the group (Tran et al., 2018).

2.5. Preparation of cytosolic and membrane fractions for Western blot analysis

Cytosolic and membrane fractions were prepared as described previously with minor modifications (Zhang et al., 2008). Animal tissues were collected and homogenized in ice-cold lysis buffer (pH 7.4) containing 25 mmol/L Tris, 250 mmol/L NaCl, 3 mmol/L ethylenediaminetetraacetic acid (EDTA), and protease inhibitor cocktail (Sigma-Aldrich, St. Louis, MO, U.S.A.) using Dounce homogenizer. The lysates were loaded onto sucrose in lysis buffer and centrifuged at 1600 × *g* for 15 min; the supernatant above the sucrose gradient was utilized as the cytosolic fraction after centrifugation at 150,000 × *g* for 30 min at 4 °C. The resulting pellets were resuspended with lysis buffer containing 1% Triton X-100 and used as the membrane fraction (Dang et al., 2016).

2.6. Western blot analysis

Hypothalamic tissues were lysed in buffer containing a 200 mM Tris–HCl (pH 6.8), 1% SDS, 5 mM EGTA, 5 mM EDTA, 10% glycerol, 1 × phosphatase inhibitor cocktail I (Sigma-Aldrich, St. Louis, MO, U.S.A.), and 1 × protease inhibitor cocktail (Sigma-Aldrich, St. Louis, MO, U.S.A.). Lysate was centrifuged at 12,000 × *g* for 30 min, and the supernatant fraction was used for Western blot analysis as described previously (Shin et al., 2014, 2012). Proteins (20 μg/lane) were separated by 8% or 10% sodium dodecyl sulfate-polyacrylamide gel electrophoresis (PAGE) and transferred onto PVDF membranes. Following transfer, the membranes were preincubated with 5% non-fat milk for 30 min, and incubated overnight at 4 °C with primary antibody against 5-HT_{1A}R (1:2000; Abcam, Cambridge, UK), PKCα (1:70,000; Santa Cruz Biotechnology), PKCβI (1:70,000; Santa Cruz Biotechnology), PKCβII (1:5000; Santa Cruz Biotechnology), PKCζ (1:10,000; Santa Cruz Biotechnology), PKCδ (1:10,000; Santa Cruz Biotechnology), p-PKCδ at Tyr311 (1:500; Santa Cruz Biotechnology), p47phox (1:500; EMD Millipore, Temecula, MA, U.S.A.), p-p47phox at Ser345 (1:1000; Sigma-Aldrich, St. Louis, MO, U.S.A.), Bcl-2 (1:1000; Santa Cruz Biotechnology), Bcl-xL (1:1000; Cell Signaling Technology), Bax (1:1000; Santa Cruz Biotechnology), cleaved caspase-3 (1:1000; Cell Signaling Technology), caspase-3 (1:5000; Cell Signaling Technology), ionized calcium binding adaptor molecule 1 (Iba-1, 1:500; Abcam, Cambridge, UK), glial fibrillary acidic protein (GFAP, 1:500; Santa Cruz Biotechnology), interleukine-6 (IL-6, 1:1000; Abcam, Cambridge, UK), interferon gamma (IFN-γ, 1:5000; Bio-Rad laboratories, CA, U.S.A), tumor necrosis factor alpha (TNF-α, 1:500; R&D Systems, Mineapolis, MN, U.S.A), cyclooxygenase-2 (COX-2, 1:2000; Santa Cruz Biotechnology), Na^+/K^+-ATPase α1 subunit (1:1000; Abcam, Cambridge, UK), or β-actin (1:50,000; Sigma-Aldrich, St. Louis, MO, U.S.A.). Membranes were then incubated with HRP-conjugated secondary anti-rabbit IgG (1:1000, GE healthcare, Piscataway, NJ, U.S.A.) or anti-mouse IgG (1:1000, Sigma-Aldrich) for 2 h. Subsequent visualization was performed using an enhanced chemiluminescence system (ECL plus®, GE Healthcare, Arlington Heights, IL, U.S.A.). Relative intensities of the bands were quantified by PhotoCapt MW (version 10.01 for Windows; Vilber Lourmat, Marne la Vallée, France), and then normalized to the intensity of β-actin (whole lysate or cytosolic fraction) or Na^+/K^+-ATPase α1 subunit (membrane fraction) (Shin et al., 2014; Tran et al., 2017).

2.7. Immunoprecipitation

Immunoprecipitation was performed as described previously (Dang et al., 2017a) using protein G-sepharose (GE Healthcare, Piscataway, NJ, U.S.A.). Hypothalamic tissues were homogenized in lysis buffer for 1 min on ice and centrifuged at 12,000 × *g* for 20 min at 4 °C to remove particulate matter. The supernatant fractions were transferred to new tubes in 1-ml aliquots and pre-cleared by the addition of 50 μl of protein G-sepharose suspension (GE Healthcare) to each tube, gentle mixing for 1 h at 4 °C, and centrifugation at 12,000 × *g* for 20 s. Five hundred microliter portions of the pre-cleared supernatant fractions were then removed to new tubes and incubated with 5 μg of an antibody specific for PKCδ (1:1000; Santa Cruz Biotechnology, Santa Cruz, CA, U.S.A) or p47phox (1:500; EMD Millipore, Temecula, MA, U.S.A.) for 1 h at 4 °C to allow the formation of immune complexes.

To precipitate the immune complexes, 50 μl of protein G-sepharose suspension was added to each tube, and the tubes were incubated for 5 h at 4 °C. The immune complexes bound to sepharose beads were recovered by centrifugation and washed three times with wash buffer to remove the excess cytosolic fraction.

For analysis, the precipitated beads were mixed with SDS-PAGE sample buffer and heated for 10 min at 95 °C. The dissociated proteins were then resolved by 10% SDS-PAGE and detected by immunoblotting with an antibody specific for 5-HT_{1A}R (1:1000; Abcam, Cambridge, UK) or PKCδ (1:1000; Santa Cruz Biotechnology, Santa Cruz, CA, U.S.A).

2.8. Reverse transcription and polymerase chain reaction (RT-PCR)

Expressions of the 5-HT_{1A} was assessed using quantitative RT–PCR to analyze mRNA levels, as described previously (Dang et al., 2017a). Total RNA was isolated from hypothalamic tissues using an RNeasy Mini Kit (Qiagen, Valencia, CA, U.S.A.) according to the manufacturer's instructions. Reverse transcription reactions were carried out using the RNA to

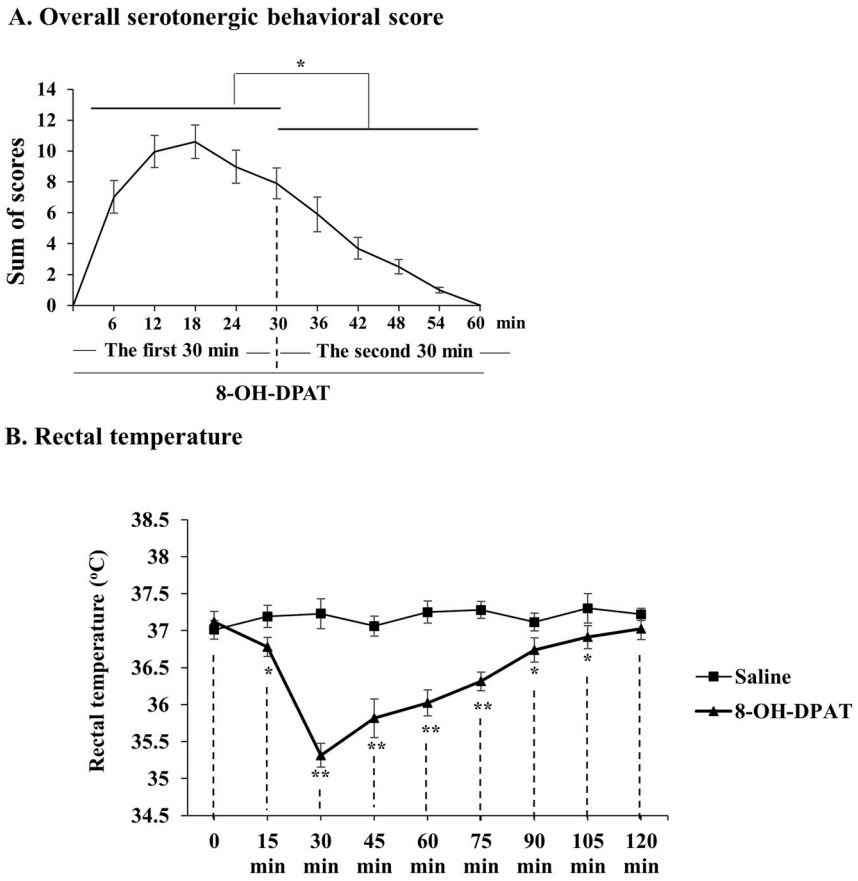

Fig. 1. 8-OH-DPAT (2 mg/kg, i.p.)-induced serotonergic behaviors (A) and hypothermia (B) in mice. Each value is the mean ± SEM of six animals. *P < 0.05, **P < 0.01 vs. mice treated with saline (ANOVA with repeated measures).

cDNA EcoDry Premix (Clontech, Palo Alto, CA, U.S.A.) with a 1-h incubation at 42 °C. PCR amplification was performed using 25 cycles of denaturation at 94 °C for 1 min, annealing at 60 °C for 2 min, and extension at 72 °C for 1 min. The primer sequences, predicted product sizes, and GenBank accession numbers (where available) for the amplified genes were as follows: mouse 5-HT_{1A}R (196 bp), 5′-GAC TGC CAC CCT CTG CCC TAT ATC-3′ (forward) and 5′-TCA GCA AGG CAA ACA ATT CCA G-3′ (reverse); and glyceraldehyde 3-phosphate dehydrogenase (GAPDH; 450 bp), 5′-ACC ACA GTC CAT GCC ATC-3′ (forward) and 5′-TCC ACC ACC CTG TTG CTG TA-3′ (reverse). PCR products were separated on 2% agarose gels containing ethidium bromide and visualized under ultraviolet light. Quantitative analysis of RNA was performed using PhotoCapt MW (version 10.01 for Windows; Vilber Lourmat).

2.9. Determination of serotonin (5-HT) and 5-hydroxyindoleacetic acid (5-HIAA) by HPLC

Mice were sacrificed by cervical dislocation, and the brains were removed. The hypothalamus was dissected, immediately frozen on dry ice, and stored at −70 °C before assays were performed. Tissues were weighed, ultrasonicated in 10% perchloric acid, and centrifuged at 20,000 × *g* for 10 min. The levels of 5-HT and its metabolite 5-HIAA were determined by HPLC coupled with an electrochemical detector, as described previously (Shin et al., 2014; Wang et al., 2012). Supernatant aliquots (20 µl) were injected into an HPLC equipped with a C18 column with 3 µm particle size (Waters). The mobile phase was comprised of 26 ml of acetonitrile, 21 ml of tetrahydrofuran, and 960 ml of 0.15 M monochloroacetic acid (pH 3.0) containing 50 mg/l of EDTA and 200 mg/ml of sodium octyl sulfate. The amount of 5-HT was determined by comparison of peak areas of tissue samples with standard, and was expressed in ng/g of wet tissue.

2.10. Determination of reactive oxygen species (ROS)

ROS formation in the hypothalamus was assessed by measuring the conversion from 2′,7′-dichlorofluorescin diacetate (DCFH-DA) to dichlorofluorescin (DCF) (Nguyen et al., 2015). Tissue homogenates were added to a tube containing 2 ml of phosphate-buffered saline (PBS) with 10 nmol of DCFH-DA, dissolved in methanol. The mixture was incubated at 37 °C for 3 h, and then fluorescence was measured at 480 nm excitation and 525 nm emission. DCF was used as a standard.

2.11. Determination of 4-hydroxynonenal (4-HNE)

The amount of lipid peroxidation was determined by measuring the level of 4-hydroxynonenal (4-HNE) using the OxiSelect™ HNE adduct ELISA kit (Cell Biolabs, Inc., San Diego, CA, U.S.A.) according to the manufacturer's instructions. 100 µl of hypothalamic homogenate at a protein concentration of 10 µg/ml was incubated in 96-well protein binding plates at 4 °C overnight. After protein adsorption, 4-HNE adducts in each well were labeled with HNE antibody, followed by HRP-conjugated secondary antibody. Colorimetric development was then performed with substrate solution. Absorbance was recorded at 450 nm using a microplate reader (Molecular Devices Inc., Sunnyvale, CA, U.S.A.), and an amount of 4-HNE adduct in each sample was calculated from the standard curve for 4-HNE-BSA (Shin et al., 2014).

2.12. Determination of protein carbonyl

The extent of protein oxidation was assessed by measuring the content of protein carbonyl groups, which was determined spectrophotometrically with the 2,4-dinitrophenylhydrazine (DNPH)-labeling procedure (Shin et al., 2012) as described by Oliver et al. (1987). The

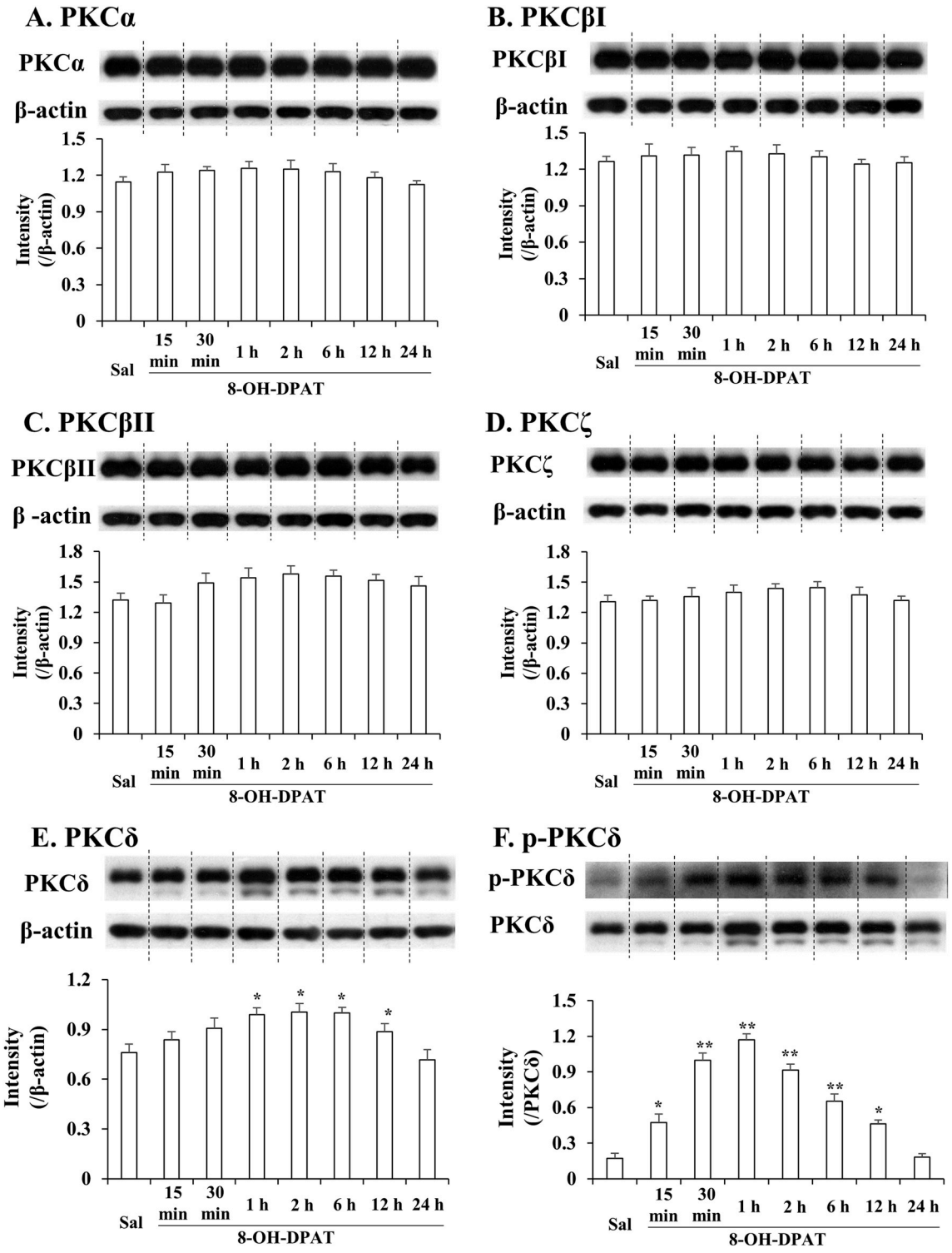

Fig. 2. Changes in the expression of PKC isoforms, and PKCδ phosphorylation 15 min, 30 min, 1 h, 2 h, 6 h, 12 h and 24 h after the 8-OH-DPAT treatment in the hypothalamus of mice. Sal = Saline. 8-OH-DPAT-induced changes in PKCα (A), PKCβI (B), PKCβII (C), PKCξ (D), PKCδ (E), and PKCδ phosphorylation (F). Each value is the mean ± SEM of six animals. *P < 0.05, **P < 0.01 vs. mice treated with saline (one-way ANOVA followed by Fisher's LSD pairwise comparisons).

results are expressed as nmol of DNPH incorporated/mg protein based on the extinction coefficient for aliphatic hydrazones of 21 mM^{-1} cm^{-1}. Protein was measured using the Pierce 660 nm Protein Assay™ reagent (Thermo Scientific, Rockford, IL, U.S.A.).

2.13. Statistical analyses

Data were analyzed using IBM SPSS ver. 21.0 (IBM, Chicago, IL, U.S.A.). One-way analysis of variance (ANOVA) was employed for statistical analyses. *Post-hoc* Fisher's least significant difference (LSD) pairwise comparison tests were then conducted. Time-dependent changes in serotonergic behavioral scores were analyzed by ANOVA with repeated measures. P-values < 0.05 were considered to be significant.

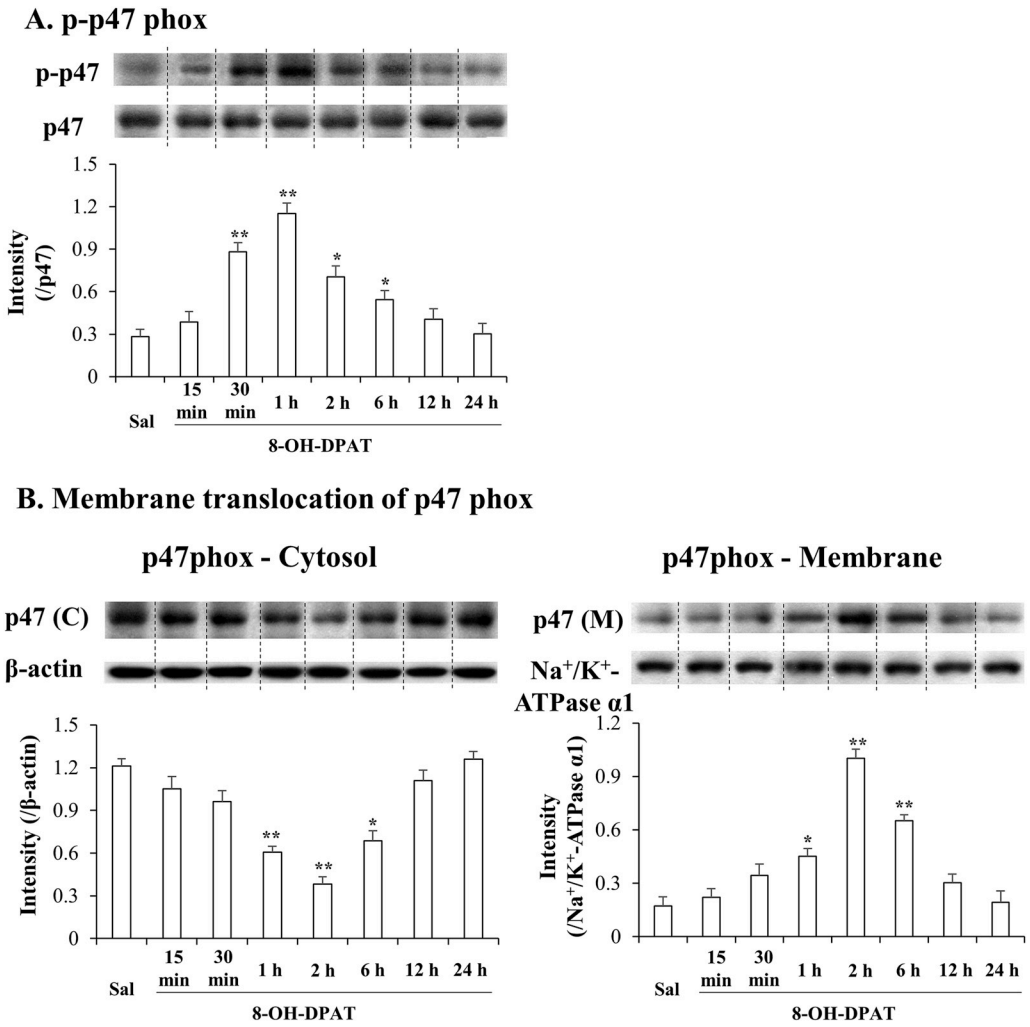

Fig. 3. Changes in the phosphorylation and membrane translocation of p47phox 15 min, 30 min, 1 h, 2 h, 6 h, 12 h and 24 h after the 8-OH-DPAT treatment in the hypothalamus of mice. Sal = Saline. 8-OH-DPAT-induced changes in the phosphorylation (A) and membrane translocation (B) of p47phox. Each value is the mean ± SEM of six animals. *P < 0.05, **P < 0.01 vs. mice treated with saline (one-way ANOVA followed by Fisher's LSD pairwise comparisons).

3. Results

3.1. Overall serotonergic behaviors and hypothermia induced by 8-OH-DPAT in mice

As shown in Supplementary Fig. S1, 8-OH-DPAT induced a broad spectrum of serotonergic behavioral response. The onset of overall serotonergic behaviors occurred within 6 min of 8-OH-DPAT administration and lasted for about 60 min. Importantly, 8-OH-DPAT-induced serotonergic behaviors mainly occurred within the first 30 min (P < 0.05 vs. the second 30 min) after the 8-OH-DPAT treatment (Fig. 1A).

Changes in body-core temperature were used to estimate autonomic dysfunction in the serotonin syndrome. As shown in Fig. 1B, initial hypothermia was observed 15 min post-8-OH-DPAT (P < 0.05), while maximal hypothermia was noted 30 min post-8-OH-DPAT (*P < 0.01*). 8-OH-DPAT-induced hypothermia lasted for at least 105 min.

3.2. Treatment with 8-OH-DPAT resulted in a selective increase in PKCδ expression over other PKC isoforms, and a significant phosphorylation of PKCδ in the hypothalamus of mice

As shown in Fig. 2A–Ehttp://link.springer.com/article/10.1007%2Fs00204-015-1516-7 - Fig. 1, PKCα, βI, βII, ζ, and δ expressions were examined 15 min, 30 min, 1 h, 2 h, 6 h, 12 h and 24 h after the 8-OH-DPAT treatment in WT mice. Treatment with 8-OH-DPAT resulted in a specific induction in PKCδ in WT mice, although no significant difference was observed in the expression of other subtypes of PKC. 8-OH-DPAT induced an initial increase in PKCδ was observed 1 h (P < 0.05) later, and this increase lasted for 12 h (P < 0.05 vs. Saline). More importantly, 8-OH-DPAT-induced initial phosphorylation of PKCδ was observed 30 min (P < 0.01) later, and it remains elevated for 12 h (P < 0.05) (Fig. 2F).

3.3. 8-OH-DPAT treatment significantly facilitated phosphorylation and membrane translocation of p47phox in the hypothalamus of wild-type mice

As shown in Fig. 3http://link.springer.com/article/10.1007%2Fs00204-015-1516-7 - Fig. 1, we examined phosphorylation (Fig. 3A) and membrane translocation (Fig. 3B) of p47phox 15 min, 30 min, 1 h, 2 h, 6 h, 12 h and 24 h after the 8-OH-DPAT treatment in WT mice. 8-OH-DPAT-induced p47phox phosphorylation was most pronounced 1 h later (Fig. 3A), while membrane translocation of p47phox was most evident 2 h later (Fig. 3B).

3.4. 8-OH-DPAT treatment significantly increased PHOX activity and oxidative parameters in the hypothalamus of mice

We investigated whether 8-OH-DPAT treatment affects PHOX

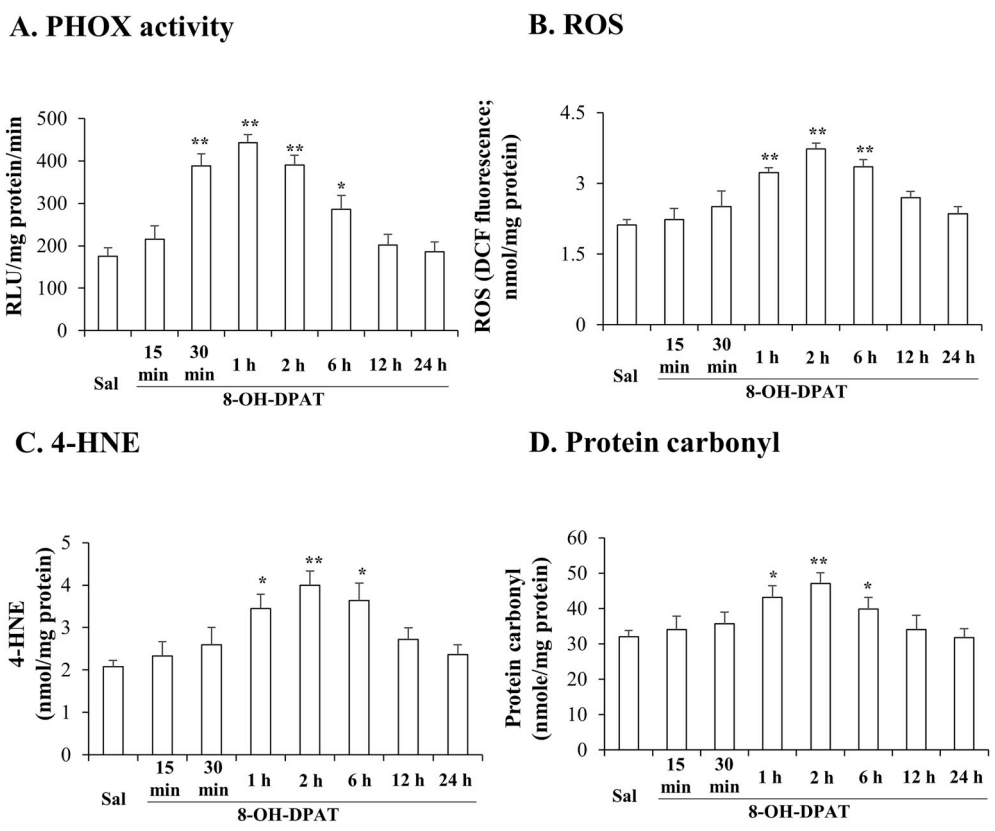

Fig. 4. Changes in NADPH oxidase (PHOX) activity and oxidative parameters 15 min, 30 min, 1 h, 2 h, 6 h, 12 h and 24 h after the 8-OH-DPAT treatment in the hypothalamus of mice. Sal = Saline. A. Changes in PHOX activity. B. Changes in reactive oxygen species (ROS) formation. C. Changes in 4-hydrononenal (4-HNE). D. Changes in protein carbonyl. Each value is the mean ± SEM of six animals. *P < 0.05, **P < 0.01 vs. mice treated with saline (one-way ANOVA followed by Fisher's LSD pairwise comparisons).

activity. As shown in Fig. 4A, 8-OH-DPAT induced an initial increase in PHOX activity 30 min (P < 0.01) later, and this increase lasted for 6 h (P < 0.05). The maximal increase appeared to be observed 1 h (P < 0.01 vs. saline) after the 8-OH-DPAT administration.

Similarly, treatment with 8-OH-DPAT resulted in initial increases in reactive oxygen species (ROS) level (P < 0.01), 4-hydroxynonenal (4-HNE), a parameter of lipid peroxidation (P < 0.05), and protein carbonyl as a parameter of protein oxidation (P < 0.05) 1 h later (Fig. 4 B – D). The maximal increases appeared to be occurred 2 h later (ROS, 4-HNE, and protein carbonyl; P < 0.01). These increases lasted for 6 h (ROS: P < 0.01, 4-HNE: P < 0.05, protein carbonyl: P < 0.05).

3.5. Effects of apocynin, rottlerin or WAY100635 on the 8-OH-DPAT-induced interaction (co-immunoprecipitation) between PKCδ and 5-HT$_{1A}$R in the hypothalamus of mice

In order to assess the interaction between PKCδ and 5-HT$_{1A}$R, we conducted an immuno-precipitation study. As shown in Fig. 5A, 8-OH-DPAT treatment significantly increased co-immunoprecipitation between PKCδ and 5-HT$_{1A}$R. The association occurred rapidly 15 min (P < 0.05), maximally 30 min–1 h (P < 0.01), and remained elevated 2 h (P < 0.05) later (Fig. 5A).

We next examined the effects of apocynin, rottlerin, or WAY100635 on the interaction between PKCδ and 5-HT$_{1A}$R 1 h after the 8-OH-DPAT treatment in WT mice. 8-OH-DPAT-induced interaction of PKCδ and 5-HT$_{1A}$R was significantly attenuated by apocynin (P < 0.01), rottlerin (P < 0.01), or WAY100635 (P < 0.01) (Fig. 5B).

3.6. Effects of apocynin, rottlerin or WAY100635 on the 8-OH-DPAT-induced interaction (co-immunoprecipitation) between p47phox and 5-HT$_{1A}$R in the hypothalamus of mice

As shown in Fig. 6A, 8-OH-DPAT treatment significantly increased co-immunoprecipitation between p47phox and 5-HT$_{1A}$R. The association occurred rapidly 15 min (P < 0.05), maximally 1 h (P < 0.01) and remains elevated 6 h later (P < 0.05) later.

We next investigated the effects of apocynin, rottlerin, or WAY100635 on the interaction of p47phox and 5-HT$_{1A}$R induced by 8-OH-DPAT. The interaction of p47phox and 5-HT$_{1A}$R was significantly attenuated by apocynin (P < 0.05), rottlerin (P < 0.05) or WAY100635 (P < 0.01) (Fig. 6B).

3.7. Effects of apocynin, rottlerin or WAY100635 on the 8-OH-DPAT-induced interaction (co-immunoprecipitation) between p47phox and PKCδ in the hypothalamus of mice

As shown in Fig. 7A, 8-OH-DPAT treatment significantly increased co-immunoprecipitation between p47phox and PKCδ. The association occurred initially 30 min (P < 0.05), maximally 1 h (P < 0.01) and remained elevated 6 h later (P < 0.05).

We also examined the effects of apocynin, rottlerin, or WAY100635 on the 8-OH-DPAT-induced interaction of p47phox and PKCδ. This interaction of p47phox and PKCδ was significantly attenuated by apocynin (P < 0.01), rottlerin (P < 0.01) or WAY100635 (P < 0.05) (Fig. 7B).

3.8. Effects of apocynin, rottlerin, or WAY100635 on the 8-OH-DPAT-induced change in pro-inflammatory parameters (i.e., Iba-1, COX-2, IFN-γ, IL-6) in the hypothalamus of mice

Here we found for the first time that 8-OH-DPAT treatment can induce pro-inflammatory parameters. As shown in Fig. 8, 8-OH-DPAT treatment significantly increased in microglial parameter Iba-1, COX-2, IFN-γ, and IL-6. Their increases were observed 1 h or 2 h through 12 h post-8-OH-DPAT. Because the maximal induction of the pro-inflammatory parameters (Iba-1, COX-2, IFN-γ, and IL6: P < 0.05, P < 0.01, P < 0.01, and P < 0.01 vs. corresponding saline, respectively) appeared to be consistently observed 2 h post-8-OH-DPAT (Fig. 8. A, C, E, and G), we investigated effects of apocynin, rottlerin, WAY100365 in response to pro-inflammatory changes. Apocynin (Iba-

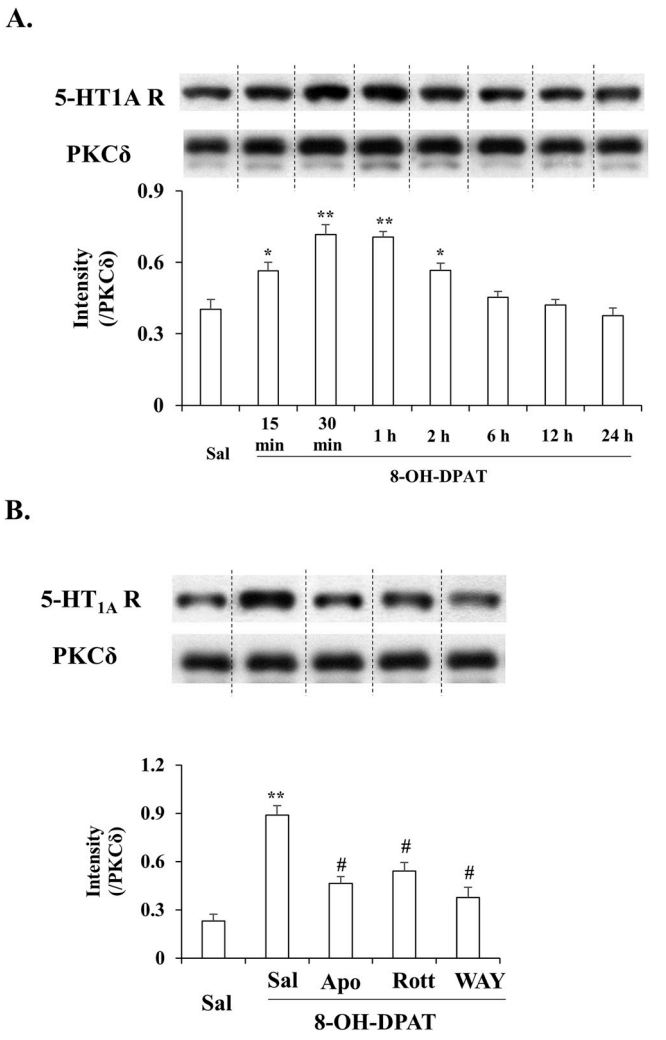

Fig. 5. Time course of changes in co-immunoprepitation of 5-HT_{1A}R and PKCδ induced by 8-OH-DPAT in the hypothalamus of mice, and effects of apocynin (Apo), rottlerin (Rott), or WAY100635 (WAY) on the interaction between PKCδ and 5-HT_{1A}R. Interaction between PKCδ and 5-HT_{1A}R 15 min, 30 min, 1 h, 2 h, 6 h, 12 h and 24 h after the 8-OH-DPAT treatment (A). Effects of apocynin (50 mg/kg, i.p.), rottlerin (3 μg, i.c.v/brain) or WAY100635 (1 mg/kg, i.p.) on the interaction between PKCδ and 5-HT_{1A}R (B). Sal = Saline. Each value is the mean ± SEM of six animals. $^{*}P < 0.05$, $^{**}P < 0.01$ vs. corresponding saline. $^{\#}P < 0.01$ vs. saline with 8-OH-DPAT (one-way ANOVA followed by Fisher's LSD pairwise comparisons).

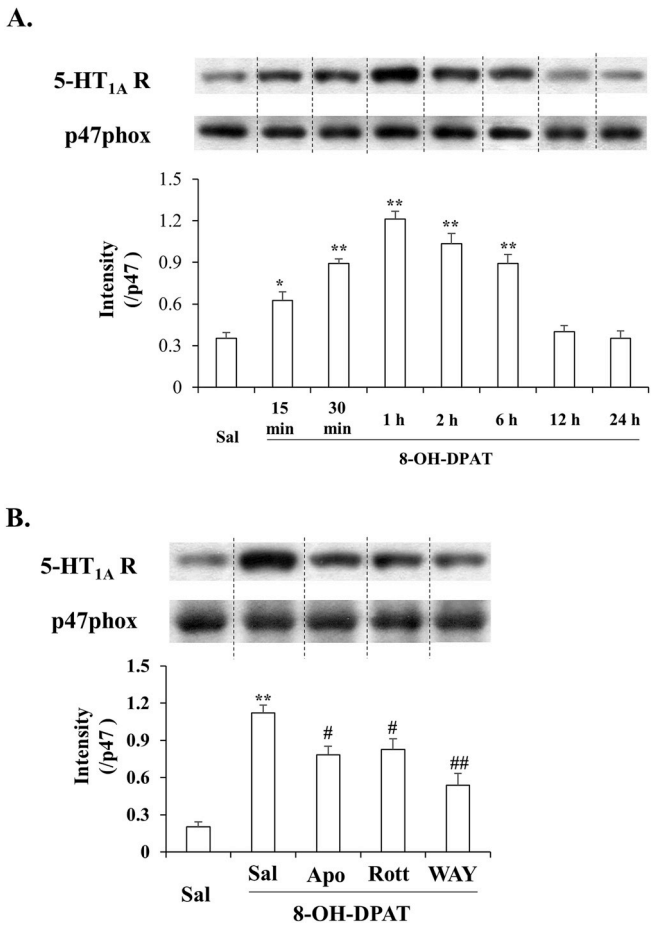

Fig. 6. Time course of changes in co-immunoprepitation of 5-HT_{1A}R and p47phox induced by 8-OH-DPAT in the hypothalamus of mice, and effects of apocynin (Apo), rottlerin (Rott), or WAY100635 (WAY) on the interaction between 5-HT_{1A}R and p47phox. Interaction between 5-HT_{1A}R and p47phox 15 min, 30 min, 1 h, 2 h, 6 h, 12 h and 24 h after the 8-OH-DPAT treatment (A). Effects of apocynin (50 mg/kg, i.p.), rottlerin (3 μg, i.c.v/brain) or WAY100635 (1 mg/kg, i.p.) on the interaction between 5-HT_{1A}R and p47phox (B). Sal = Saline. Each value is the mean ± SEM of six animals. $^{*}P < 0.05$, $^{**}P < 0.01$ vs. corresponding saline. $^{\#}P < 0.05$, $^{\#\#}P < 0.01$ vs. saline with 8-OH-DPAT (one-way ANOVA followed by Fisher's LSD pairwise comparisons).

1, COX-2, IFN-γ, IL-6: $P < 0.05$, $P < 0.01$, $P < 0.05$, and $P < 0.01$, respectively), rottlerin (Iba-1, COX-2, IFN-γ, IL-6: $P < 0.05$, $P < 0.01$, $P < 0.05$, and $P < 0.01$, respectively), and WAY100365 (Iba-1, COX-2, IFN-γ, IL-6: $P < 0.05$, $P < 0.01$, $P < 0.05$, and $P < 0.01$, respectively) significantly attenuated against 8-OH-DPAT-induced increases in Iba-1, COX-2, IFN-γ, IL-6 in the hypothalamus of mice. However, neither astrocytic parameter GFAP nor TNF-α expression significantly changed by 8-OH-DPAT (Fig. 8 I and J).

3.9. Effects of apocynin, rottlerin, or WAY100635 on the 8-OH-DPAT-induced change in anti-apoptotic (i.e., Bcl-2 and Bcl-xL) and pro-apoptotic (i.e., Bax and cleaved caspase- 3) factors in the hypothalamus of mice

We observed that 8-OH-DPAT treatment down-regulates anti-apoptotic parameters, while it up-regulates pro-apoptotic parameters. As shown in Fig. 9, Bcl-2 ($P < 0.05$), Bcl-xL ($P < 0.05$), Bax ($P < 0.05$), and cleaved caspase-3 ($P < 0.05$) were initially changed 1 h post-8-OH-DPAT. Maximal changes in Bcl-2 ($P < 0.01$), Bcl-xL ($P < 0.01$), Bax ($P < 0.01$), and cleaved caspase-3 ($P < 0.01$) were consistently occurred 2 h post-8-OH-DPAT. The change of these parameters were still observed 6–12 h post-8-OH-DPAT (Fig. 9A, C, E, and G). We then applied apocynin, rettlerin or WAY100365 2 h post-8-OH-DPAT to investigate whether inhibition of PHOX, PKCδ or 5-HT_{1A}R affects anti-apoptotic and pro-apoptotic parameters (Fig. 9B, D, F and H). Apocynin (Bcl-2, Bcl-xL, Bax, and cleaved caspase-3: $P < 0.01$, $P < 0.05$, $P < 0.01$, and $P < 0.05$, respectively), rottlerin (Bcl-2, Bcl-xL, Bax, and cleaved caspase-3: $P < 0.01$, $P < 0.05$, $P < 0.01$, and $P < 0.05$, respectively), and WAY100365 (Bcl-2, Bcl-xL, Bax, and cleaved caspase-3: $P < 0.01$, $P < 0.05$, $P < 0.01$, and $P < 0.05$, respectively) significantly attenuated against decreases in Bcl-2 and Bcl-xL and increases in Bax and cleaved caspase-3 induced by 8-OH-DPAT.

3.10. Effects of apocynin, rottlerin, or WAY100635 on the 8-OH-DPAT-induced change in the 5-HT turnover rate in the hypothalamus of WT, p47phox KO, and PKCδ KO mice

As shown in Fig. 10A and B, 8-OH-DPAT treatment significantly increased 5-HT level ($P < 0.01$) and 5-HT turnover rate ($P < 0.01$) in WT mice. These increases were significantly attenuated by apocynin (5-HT: $P < 0.01$, 5-HT turnover rate: $P < 0.05$), rottlerin (5-HT:

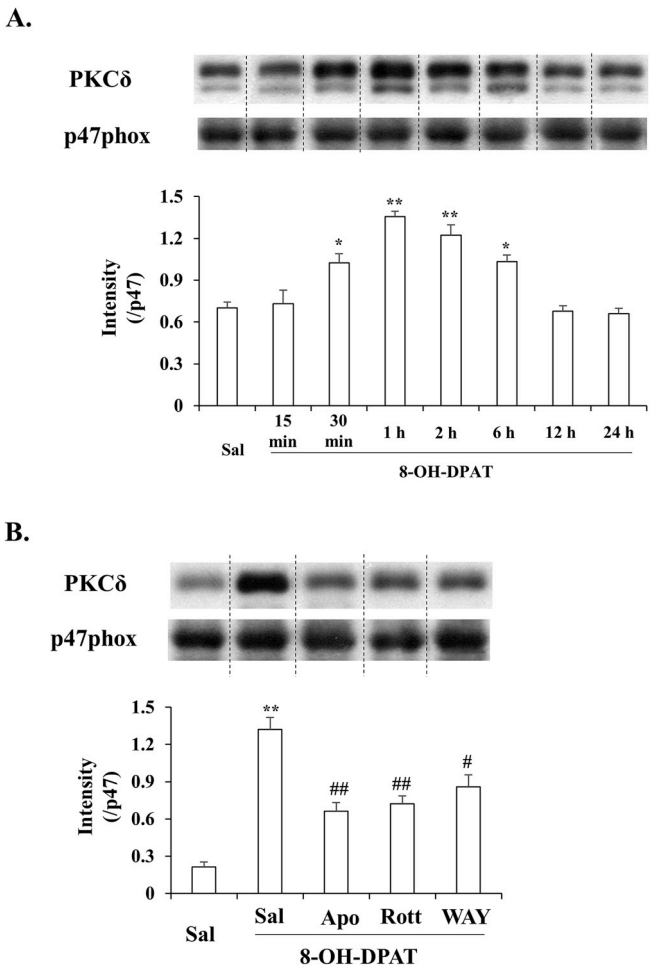

Fig. 7. Time course of changes in co-immunoprepitation of PKCδ and p47phox induced by 8-OH-DPAT in the hypothalamus of mice, and effects of apocynin (Apo), rottlerin (Rott), or WAY100635 (WAY) on the interaction between PKCδ and p47phox. Interaction between PKCδ and p47phox 15 min, 30 min, 1 h, 2 h, 6 h, 12 h and 24 h after the 8-OH-DPAT treatment (A). Effects of apocynin (50 mg/kg, i.p.), rottlerin (3 μg, i.c.v/brain) or WAY100635 (1 mg/kg, i.p.) on the interaction between PKCδ and p47phox (B). Sal = Saline. Each value is the mean ± SEM of six animals. $^{*}P < 0.05$, $^{**}P < 0.01$ vs. corresponding saline. $^{\#}P < 0.05$, $^{\#\#}P < 0.01$ vs. saline with 8-OH-DPAT (one-way ANOVA followed by Fisher's LSD pairwise comparisons).

P < 0.01, 5-HT turnover rate: P < 0.05), or WAY100635 (5-HT and 5-HT turnover rate: P < 0.05, respectively) (Fig. 10A and B). Consistently, p47phox knockout (5-HT: P < 0.01, 5-HT turnover rate: P < 0.05) or PKCδ knockout (5-HT and 5-HT turnover rate: P < 0.05, respectively) significantly attenuated serotonergic impairment induced by 8-OH-DPAT. The effects of apocynin were comparable to those of genetic inhibition of p47phox against serotonergic impairment in mice. Rottlerin or WAY100635 treatment did not show any additive effects against the pharmacological activity by p47phox knockout in mice. Similarly, the effects of rottlerin were comparable to those of PKCδ knockout in response to serotonergic impairment. Apocynin or WAY100635 did not affect against the attenuation by PKCδ knockout in mice (Fig. 10A and B).

3.11. Effects of apocynin, rottlerin, or WAY100635 on the 8-OH-DPAT-induced changes in 5-HT$_{1A}$R gene expression, and p47phox phosphorylation and p47phox membrane translocation in the hypothalamus of WT, p47phox KO, or PKCδ KO mice

As shown in Fig. 11A and B, 5-HT$_{1A}$R mRNA (P < 0.01) and

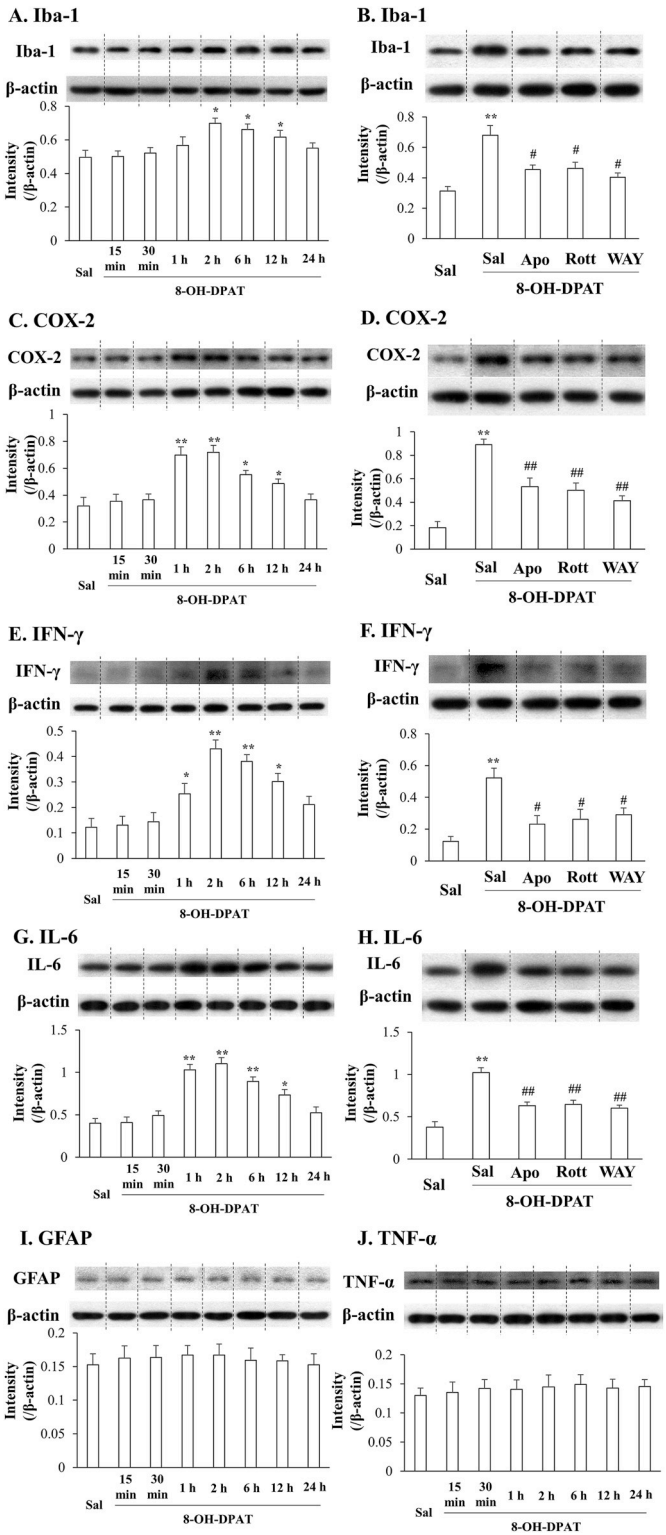

Fig. 8. Time course of changes in the expression of Iba-1, COX-2, IFN-γ, IL-6, GFAP, and TNF-α induced by 8-OH-DPAT in the hypothalamus of mice, and effect of apocynin (Apo), rottlerin (Rott), or WAY100635 (WAY) on the Iba-1, COX-2, IFN-γ, and IL-6 levels. Expressions of Iba-1 (A), COX-2 (C), IFN-γ (E), IL-6 (G), GFAP (I) and TNF-α (J) 15 min, 30 min, 1 h, 2 h, 6 h, 12 h and 24 h after the 8-OH-DPAT treatment. Effect of apocynin (50 mg/kg, i.p.), rottlerin (3 μg, i.c.v/brain) or WAY100635 (1 mg/kg, i.p.) on the Iba-1 (B), COX-2 (D), IFN-γ (F), and IL-6 (H) levels. Sal = Saline. Each value is the mean ± SEM of six animals. $^{*}P < 0.05$, $^{**}P < 0.01$ vs. corresponding saline. $^{\#}P < 0.05$, $^{\#\#}P < 0.01$ vs. saline with 8-OH-DPAT (one-way ANOVA followed by Fisher's LSD pairwise comparisons).

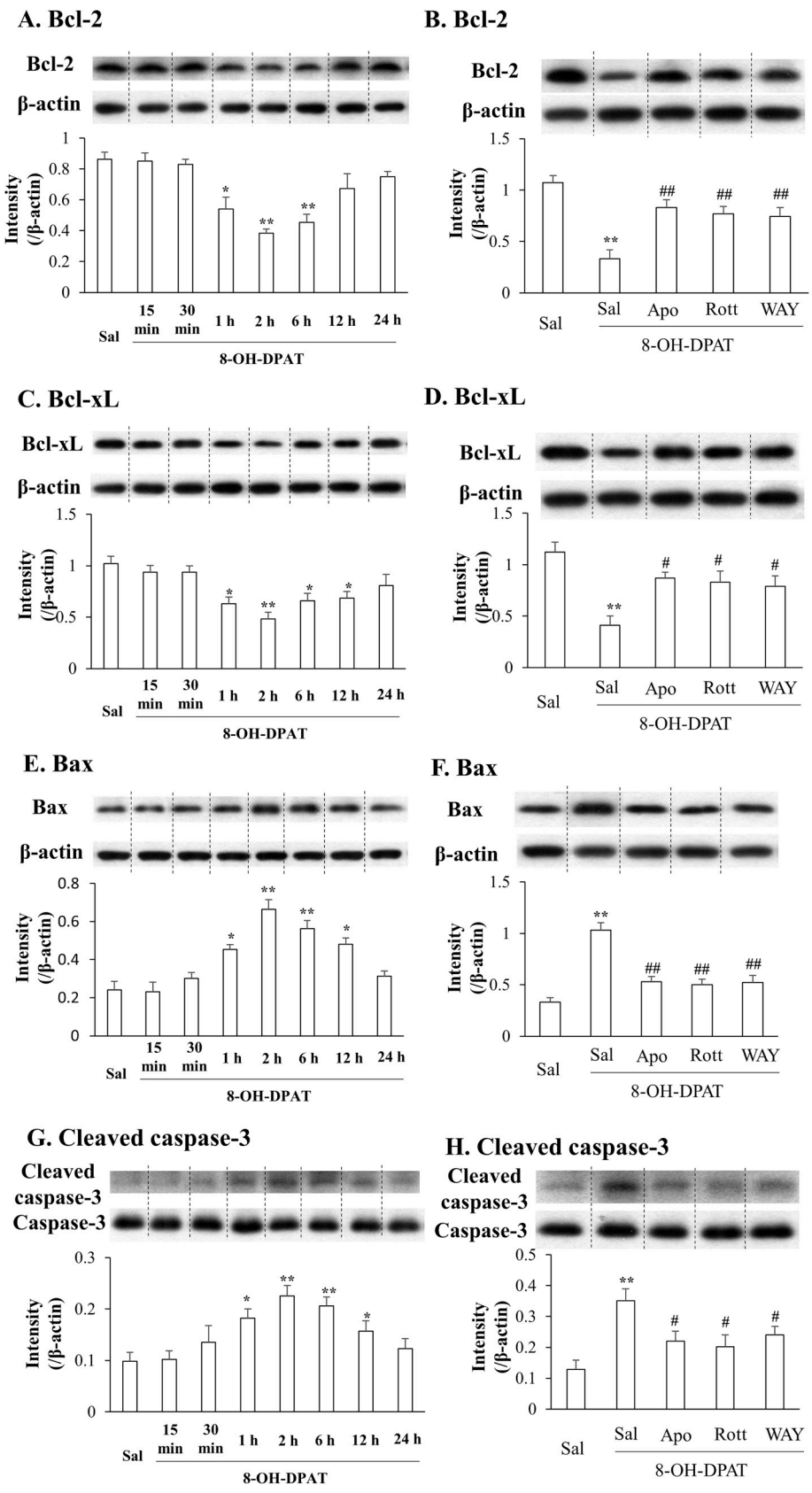

Fig. 9. Time course of changes in the expression of Bcl-2, Bcl-xL, Bax, and cleaved caspase-3 induced by 8-OH-DPAT in the hypothalamus of mice, and effect of apocynin (Apo), rottlerin (Rott), or WAY100635 (WAY) on the Bcl-2, Bcl-xL, Bax, and cleaved caspase-3 levels. Expressions of Bcl-2 (A), Bcl-xL (C), Bax (E), and cleaved caspase-3 (G) 15 min, 30 min, 1 h, 2 h, 6 h, 12 h and 24 h after the 8-OH-DPAT treatment. Effect of apocynin (50 mg/kg, i.p.), rottlerin (3 μg, i.c.v/brain) or WAY100635 (1 mg/kg, i.p.) on the Bcl-2 (B), Bcl-xL (D), Bax (F), and cleaved caspase-3 (H) levels. Sal = Saline. Each value is the mean ± SEM of six animals. $^{*}P < 0.05$, $^{**}P < 0.01$ vs. corresponding saline. $^{\#}P < 0.05$, $^{\#\#}P < 0.01$ vs. saline with 8-OH-DPAT (one-way ANOVA followed by Fisher's LSD pairwise comparisons).

protein ($P < 0.01$) expressions were significantly increased 15 min after the 8-OH-DPAT treatment. The increase in 5-HT_{1A}R expression was significantly attenuated by apocynin (mRNA: $P < 0.01$, protein: $P < 0.05$), rottlerin (mRNA: $P < 0.01$, protein: $P < 0.05$), or WAY100635 (mRNA and protein: $P < 0.01$, respectively) (Fig. 11A and B). Consistently, p47phox knockout (mRNA and protein: $P < 0.01$, respectively) or PKCδ knockout (mRNA and protein: $P < 0.01$, respectively) significantly attenuated 5-HT_{1A}R gene expression induced

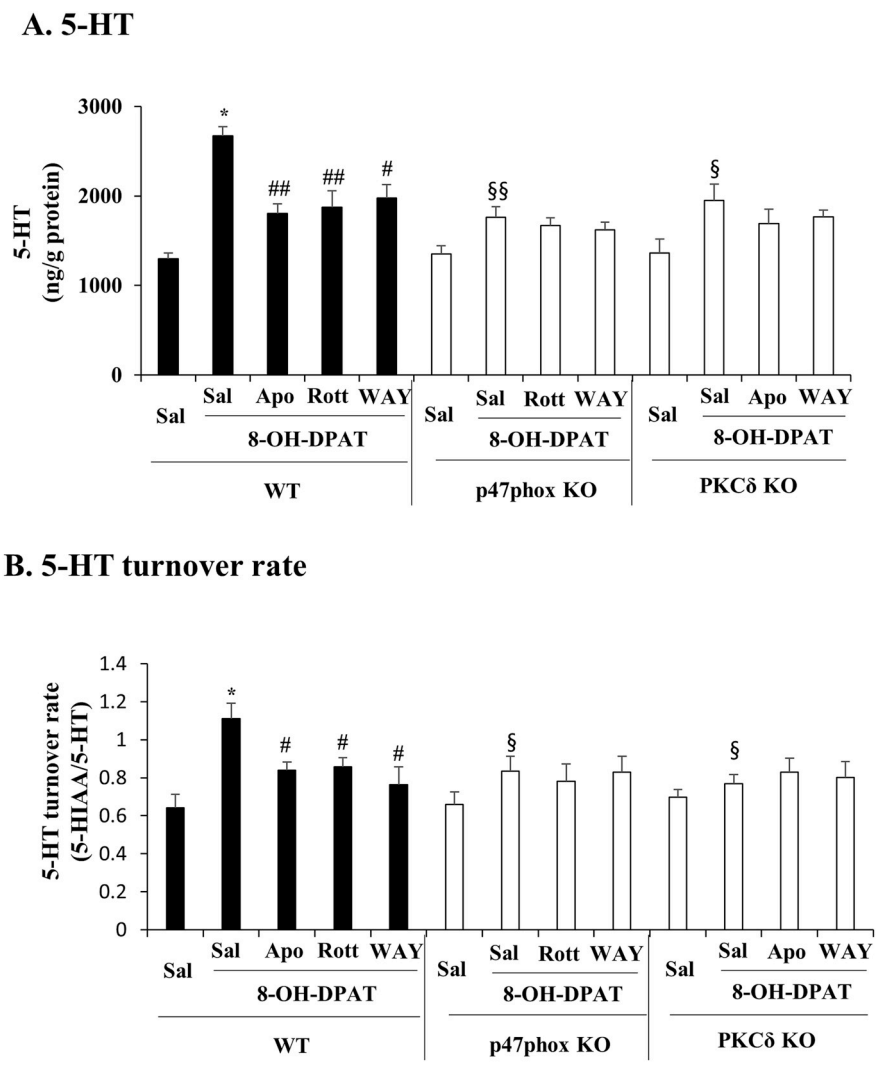

Fig. 10. Effects of apocynin (Apo), rottlerin (Rott), or WAY100635 (WAY) on the changes in 5-HT level (A) and 5-HT turnover rate (B) induced by 8-OH-DPAT in the hypothalamus of wild type (WT), p47phox KO, and PKCδ KO mice. Sal = Saline. PKCδ KO = PKCδ knockout mice. p47phox KO = p47phox knockout mice. Each value is the mean ± SEM of six animals. $^{*}P < 0.01$ vs. corresponding saline. $^{\#}P < 0.05$, $^{\#\#}P < 0.01$ vs. saline with 8-OH-DPAT. $^{\S}P < 0.05$, $^{\S\S}P < 0.01$ vs. saline with 8-OH-DPAT/WT (one-way ANOVA followed by Fisher's LSD pairwise comparisons).

by 8-OH-DPAT. The effects of apocynin were comparable to those of p47phox knockout. Rottlerin or WAY100635 treatment did not show any additive effects against the pharmacological activity by p47phox knockout in mice. Similarly, the effects of rottlerin were comparable to those of PKCδ knockout. Apocynin or WAY100635 did not affect against the attenuation by PKCδ knockout in mice (Fig. 11A and B).

As shown in Fig. 11C, 8-OH-DPAT treatment significantly increased p47phox phosphorylation ($P < 0.01$). The p47phox phosphorylation was significantly attenuated by rottlerin ($P < 0.01$) or WAY100635 ($P < 0.01$). Consistently, genetic inhibition of PKCδ significantly attenuated the p47phox phosphorylation ($P < 0.01$) induced by 8-OH-DPAT. The effects of rottlerin were comparable to those of PKCδ knockout. WAY100635 did not affect against the attenuation by PKCδ knockout (Fig. 11C).

As shown in Fig. 11D, treatment with 8-OH-DPAT resulted in a significant decrease in cytosolic p47phox expression ($P < 0.01$), while resulted in a significant increase in p47phox membrane translocation ($P < 0.01$). Rottlerin ($P < 0.01$) or WAY100635 ($P < 0.01$) treatment significantly attenuated against the membrane translocation of p47phox induced by 8-OH-DPAT. The effects of rottlerin were comparable to those of PKCδ knockout. WAY100635 treatment did not show any additional effects against the attenuation by PKCδ knockout in mice (Fig. 11D).

3.12. Effects of apocynin, rottlerin, or WAY100635 on the 8-OH-DPAT-induced changes in PHOX activity and oxidative parameters in the hypothalamus of WT, p47phox KO, and PKCδ KO mice

As shown in Fig. 12A, treatment with 8-OH-DPAT resulted in a significant increase in PHOX activity ($P < 0.01$) 1 h after the 8-OH-DPAT treatment. The increase in PHOX activity was significantly attenuated by apocynin ($P < 0.05$), rottlerin ($P < 0.05$), or WAY100635 ($P < 0.05$). Consistently, p47phox knockout ($P < 0.05$) or PKCδ knockout ($P < 0.05$) significantly attenuated PHOX activity induced by 8-OH-DPAT. The effects of apocynin were comparable to those of p47phox knockout. Rottlerin or WAY100635 treatment did not show any additive effects against the pharmacological activity by p47phox knockout in mice. Similarly, the effects of rottlerin were comparable to those of PKCδ knockout in mice. Apocynin or WAY100635 did not affect against the attenuation by PKCδ knockout in mice (Fig. 12A).

Apocynin, rottlerin or WAY100635 significantly attenuated 8-OH-DPAT-induced increases in ROS (apocynin, rottlerin, and WAY100635: $P < 0.05$, respectively), 4-HNE (apocynin, rottlerin, and WAY100635: $P < 0.05$, respectively) and protein carbonyl (apocynin, rottlerin, and WAY100635: $P < 0.05$, respectively) (Fig. 4B–D and Fig. 12B–D). Consistently, p47phox knockout (ROS, 4-HNE, and protein carbonyl:

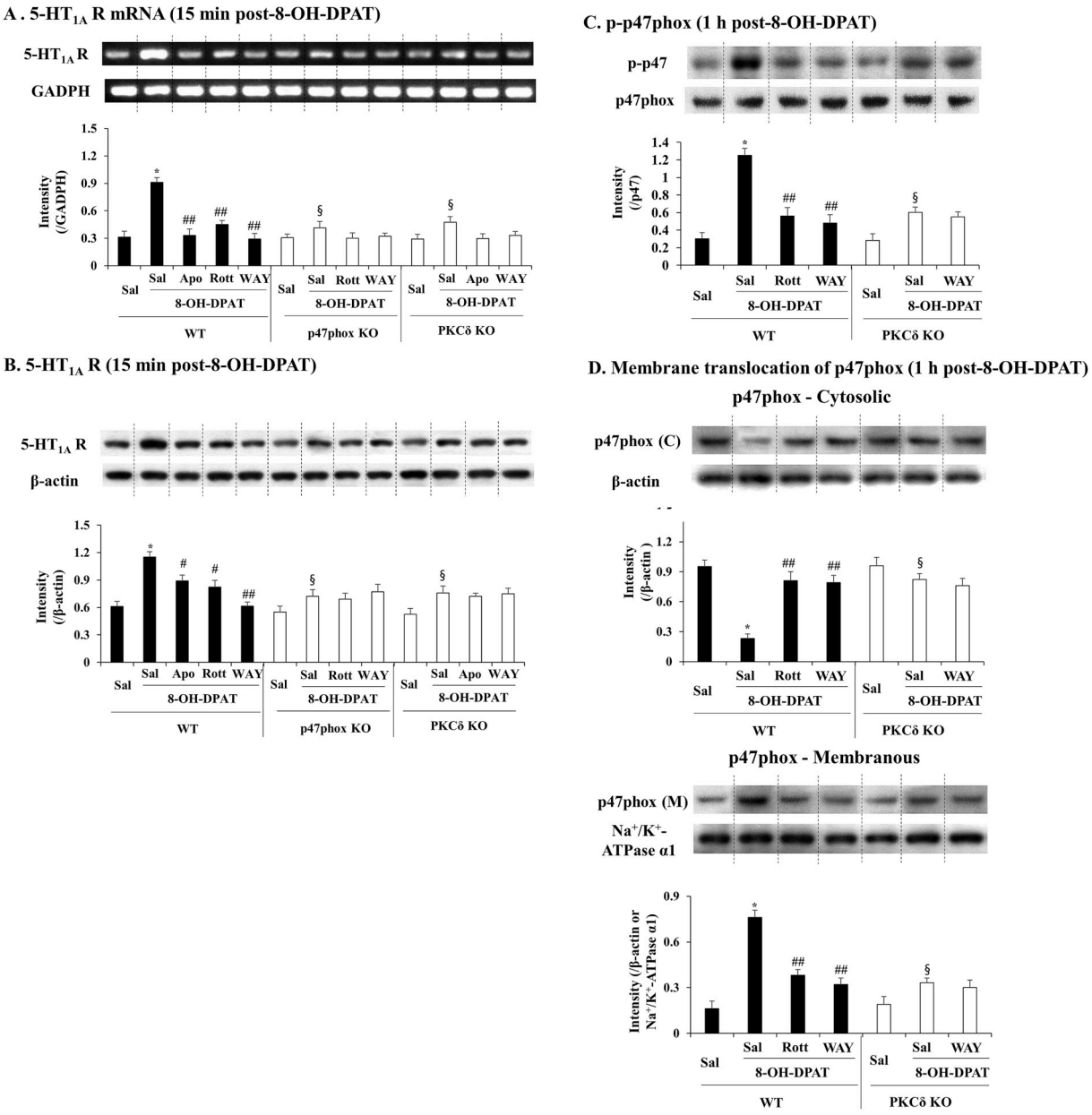

Fig. 11. Effects of apocynin (Apo), rottlerin (Rott), or WAY100635 (WAY) on the changes in 5-HT_{1A}R mRNA (A) and 5-HT_{1A}R protein expression (B), p47phox phosphorylation (C), and p47phox cytosolic and membrane expression (D) induced by 8-OH-DPAT in the hypothalamus of wild type mice (WT), p47phox KO, or PKCδ KO mice. Sal = Saline. PKCδ KO = PKCδ knockout mice. p47phox KO = p47phox knockout mice. Each value is the mean ± SEM of six animals. $^{*}P < 0.01$ vs. corresponding saline. $^{\#}P < 0.05$, $^{\#\#}P < 0.01$ vs. saline with 8-OH-DPAT. $^{\S}P < 0.01$ vs. saline with 8-OH-DPAT/WT (one-way ANOVA followed by Fisher's LSD pairwise comparisons).

$P < 0.05$, respectively) or PKCδ knockout (ROS, 4-HNE, and protein carbonyl: $P < 0.05$, respectively) significantly attenuated oxidative burdens induced by 8-OH-DPAT. The attenuation by apocynin was comparable to that by p47phox knockout. Rottlerin or WAY100635 did not show any additive effects against the attenuation by p47phox knockout. In addition, the attenuation by rottlerin was comparable to that by PKCδ knockout. WAY100635 or apocynin treatment did not show any additive effects against the attenuation by PKCδ knockout in mice (Fig. 12B–D).

3.13. Effects of WAY100635 on 8-OH-DPAT-induced changes in serotonergic behaviors and hypothermia in WT, p47phox KO, and PKCδ KO mice

Because the change in serotonergic behaviors was more pronounced in the first 30 min than the second 30 min post-8-OH-DPAT (Fig. 1A), we have focused on the first 30 min period. As presented in Fig. 13A, treatment with 8-OH-DPAT resulted in a significant increase in overall serotonergic behavioral score ($P < 0.01$). Treatment with apocynin ($P < 0.01$), rottlerin ($P < 0.01$), or WAY100635 ($P < 0.01$) significantly attenuated overall serotonergic behavioral score induced by 8-OH-DPAT. Consistently, p47phox knockout ($P < 0.01$) or PKCδ knockout ($P < 0.01$) significantly attenuated overall serotonergic behavioral score induced by 8-OH-DPAT. The effects of apocynin were comparable to those of genetic depletion of p47phox. Rottlerin or WAY100635 treatment did not show any additive effects against the pharmacological activity by p47phox knockout in mice. Similarly, the effects of rottlerin were comparable to those of PKCδ knockout. Apocynin or WAY100635 did not affect against the attenuation by PKCδ knockout in mice (Fig. 13A).

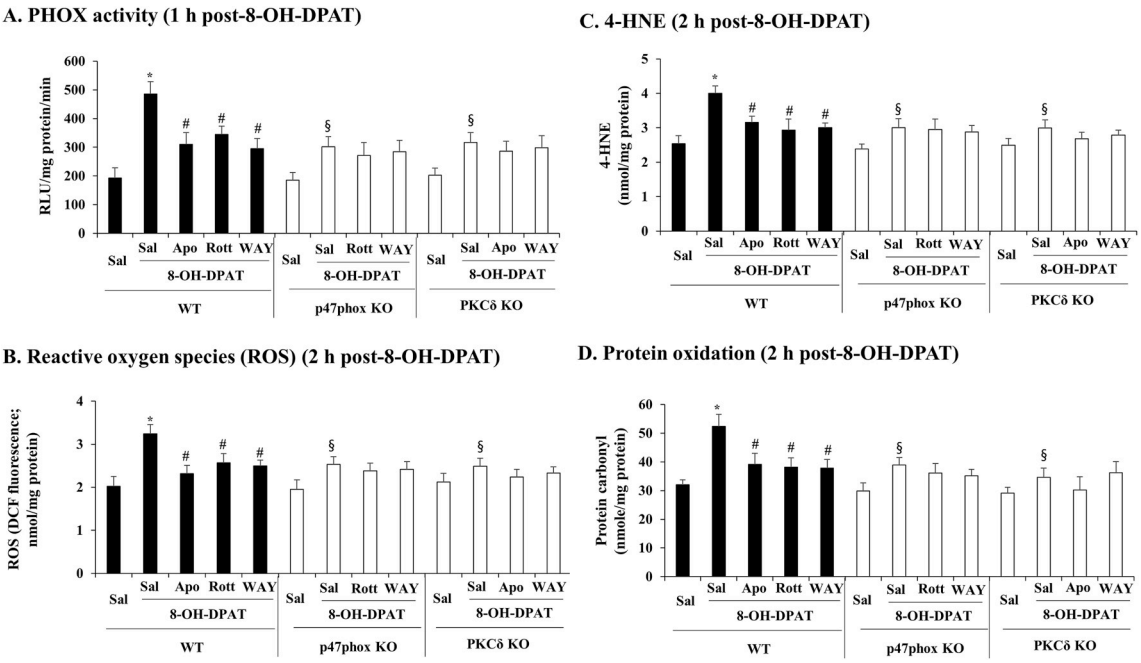

Fig. 12. Effects of apocynin (Apo), rottlerin (Rott), or WAY100635 (WAY) on the changes in 8-OH-DPAT-induced PHOX activity and oxidative parameter in the hypothalamus of wild type mice (WT), p47phox KO, and PKCδ KO mice. Changes of PHOX activity (A). Changes of reactive oxygen species (ROS) (B). Changes of 4-hydrononenal (4-HNE) (C). Changes of protein carbonyl (D). Sal = Saline. PKCδ KO = PKCδ knockout mice. p47phox KO = p47phox knockout mice. Each value is the mean ± SEM of six animals. $^{*}P < 0.01$ vs. corresponding saline. $^{\#}P < 0.05$ vs. saline with 8-OH-DPAT. $^{\S}P < 0.05$ vs. saline with 8-OH-DPAT/WT (one-way ANOVA followed by Fisher's LSD pairwise comparisons).

Since changes in rectal temperature was also more pronounced in the first 30 min than the second 30 min-post 8-OH-DPAT (Fig. 1B), we have focused on the first 30 min period. As shown in Fig. 13B, treatment with 8-OH-DPAT resulted in a significant hypothermia ($P < 0.01$). Treatment with apocynin ($P < 0.01$), rottlerin ($P < 0.01$), or WAY100635 ($P < 0.01$) significantly attenuated hypothermia induced by 8-OH-DPAT. Consistently, p47phox knockout ($P < 0.01$) or PKCδ knockout ($P < 0.01$) significantly attenuated hypothermia induced by 8-OH-DPAT. The effects of apocynin were comparable to those of p47phox knockout. Rottlerin or WAY100635 treatment did not show any additive effects against the pharmacological activity offered by p47phox knockout in mice. Similarly, the effects of rottlerin were comparable to those of PKCδ knockout. Apocynin or WAY100635 did not affect against the attenuation by PKCδ knockout in mice (Fig. 13 B).

4. Discussion

Here, we observed that 8-OH-DPAT (2 mg/kg, i.p.) initially induces phosphorylation of PKCδ. Simultaneously, PKCδ-dependent 5-HT_{1A}R activation was occurred rapidly. These initial cascades led to the activation of p47phox and resulted in PKCδ-dependent p47phox activation. In addition, 8-OH-DPAT facilitated the interaction between 5-HT_{1A}R and p47phox. These up-stream cascades possibly contribute to serotonergic behaviors in mice. Thereafter, the initial membrane translocation of p47phox occurred. Therefore, this signaling process could facilitate the oxidative, pro-inflammatory, and pro-apoptotic changes. 5-HT_{1A}R antagonist WAY100635 did not exhibit any responses against the attenuation offered by genetic inhibition of PKCδ or p47phox. 8-OH-DPAT-induced altered parameters (i.e., 5-HT turnover rate, 5-HT_{1A}R gene expression, PKCδ phosphorylation, interaction of 5-HT_{1A}R and PKCδ, p47phox phosphorylation and membrane translocation, and pro-inflammatory/pro-apoptotic changes) returned near control level within 24 h. Therefore, we suggest that initial phosphorylation of PKCδ mediates 8-OH-DPAT-induced serotonergic behaviors via 5-HT_{1A}R activation, and that inhibition of PKCδ-dependent p47phox activation (i.e., phosphorylation and membrane translocation) is important for attenuating 8-OH-DPAT-induced serotonergic behaviors (Fig. 14).

Multiple clinical and *in vivo* studies have proposed the importance of hypothalamic dysfunction in serotonin syndrome (Nisijima et al., 2000; Shioda et al., 2004; Tran et al., 2018). The abnormality in vital physiological homeostasis of serotonin syndrome might contribute to stimulation of catecholamine release in the adrenal gland and hypothalamus (Shioda et al., 2004; Watts et al., 2012). It is recognized that many symptoms of the serotonin syndrome are centrally mediated by 5-HT_{1A}R and 5-HT_{2A}R (Boyer and Shannon, 2005; Haberzettl et al., 2013), although excess serotonergic activity in the peripheral system (including adrenal gland) may also contribute to the spectrum of symptoms (e.g. vomiting, diarrhea, etc.) (Brown et al., 1996; Haberzettl et al., 2013). Although it is well-established that 5-HT cannot cross the blood-brain barrier, previous *in vivo* studies showed that central administration of 5-HT induces head shaking, forepaw treading, head weaving, hind limb abduction, tremor, hyperactivity, and backward walking (Haberzettl et al., 2013; Shimomura et al., 1981; Sloviter et al., 1978). In particular, Haberzettl et al. (2013) suggested that central mechanism is mainly involved in the induction of serotonergic behavioral responses *in vivo*. In addition, several lines of evidence suggest that the hypothalamic 5-HT level and its major metabolite, 5-HIAA, selectively increased in various models of serotonin syndrome (Nisijima, 2000; Nisijima et al., 2000; Squires et al., 2006). Recently, we have reported that dextromethorphan-induced serotonergic impairment in the hypothalamus is much more sensitive than in the hippocampus or in the prefrontal cortex (Tran et al., 2018). Furthermore, here we observed that serotonergic activity (i.e., 5-HT level and 5-HT turnover rate) in the hypothalamus is much more sensitive than in the hippocampus or in the prefrontal cortex (Supplementary Fig. S2). Therefore, we propose that the hypothalamus is a specific region for serotonergic signaling by 8-OH-DPAT.

Serotonin syndrome is a toxic state caused mainly by excess serotonin within the central nervous system, and this excess serotonin can easily be metabolized by several metabolic pathways. The majority of serotonin is catabolized by monoamine oxidase (MAO). MAO-A has the highest affinity for serotonin (Billett, 2004)http://onlinelibrary.wiley.

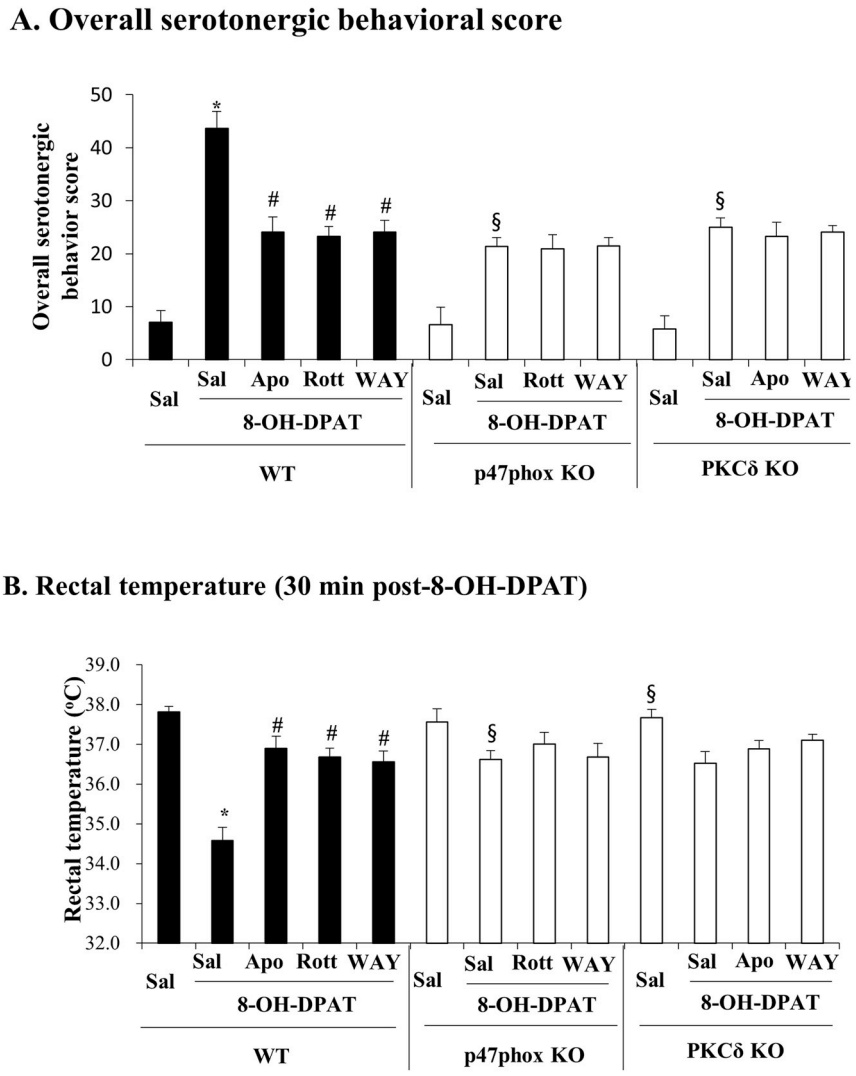

Fig. 13. Effects of apocynin (Apo), rottlerin (Rott), or WAY100635 (WAY) on the changes in 8-OH-DPAT-induced overall serotonergic behaviors (A) and hypothermia (B) in wild type mice (WT), p47phox KO, and PKCδ KO mice. Sal = Saline. PKCδ KO = PKCδ knockout mice. p47phox KO = p47phox knockout mice. Each value is the mean ± SEM of six animals. $^{*}P < 0.01$ vs. corresponding saline. $^{\#}P < 0.01$ vs. saline with 8-OH-DPAT. $^{\S}P < 0.01$ vs. saline with 8-OH-DPAT/WT (one-way ANOVA followed by Fisher's LSD pairwise comparisons).

com/doi/10.1111/j.1365-2982.2009.01370.x/full - b18. This enzyme is located in mitochondria of a wide range of cells and catalyzes oxidative deamination of several biogenic amines (Squires et al., 2006). During this process, H_2O_2 and reactive aldehydes as by-products can be generated (Squires et al., 2006). Therefore, the excess 5-HT released by 8-OH-DPAT can be a relevant source of oxidative products, and contribute to the development of oxidative damage. We observed here that 8-OH-DPAT treatment facilitates oxidative burdens in the hypothalamus, as shown by formation of HNE, protein carbonyl, and ROS. In the line with the current study, earlier investigations have also indicated that the 5-HT_{1A}R activation stimulate production of at least two oxidative parameters, such as superoxide and hydrogen peroxide (Mukhin et al., 2000). In addition, PHOX might be involved in the 5-HT_{1A}R-mediated generation of superoxide and hydrogen peroxide (Mukhin et al., 2000).

It was demonstrated that PKC is among a group of cell-signaling molecules that are sensitive targets for redox modification (Gopalakrishna and Jaken, 2000). In terms of redox-stimulated signaling, it is important to note that there is a significant overlap exists between PKC-mediated and oxidant-induced signaling responses (Gopalakrishna and Jaken, 2000). Accumulating evidence has suggested the relationship between PKCδ activation and oxidative products in *in vitro* and *in vivo* model (Dang et al., 2017b; Nitti et al., 2005; Shin et al., 2012). Domenicotti et al. (2003) demonstrated that rottlerin acts as a free radical scavenger in glutathione-depleted neuroblastoma cells, protecting them from ROS-mediated apoptosis. In this study, we demonstrated that 8-OH-DPAT-induced oxidant generation is attenuated by rottlerin or genetic inhibition of PKCδ, suggesting that PKCδ gene is a key mediator of oxidative damage induced by 8-OH-DPAT.

Earlier studies showed that 5-HT_{1A}R activates several different protein kinases. Earlier *in vitro* studies suggested that 5-HT_{1A}R activates PKC (Liu and Albert, 1991; Middleton et al., 1990; Raymond et al., 1989). It is recognized that PKC is involved in regulation of 5-HTR activity (Anji et al., 2001; Ramamoorthy et al., 1998). Recently, we have reported that up-regulation of 5-HT_{1A}R via activation of PKCδ mediates dextromethorphan-induced serotonergic behaviors (Tran et al., 2018). Consistently, the current study demonstrates that interaction between PKCδ and 5-HT_{1A}R is required for 8-OH-DPAT-induced serotonergic behaviors. Consequently, we also showed that inhibition of PKCδ attenuates serotonergic behaviors, hypothermia, and increased serotonin turnover rate induced by 8-OH-DPAT, indicating that PKCδ plays a critical role in mediating 8-OH-DPAT-induced serotonergic impairments.

Previous studies have demonstrated that activation of PHOX

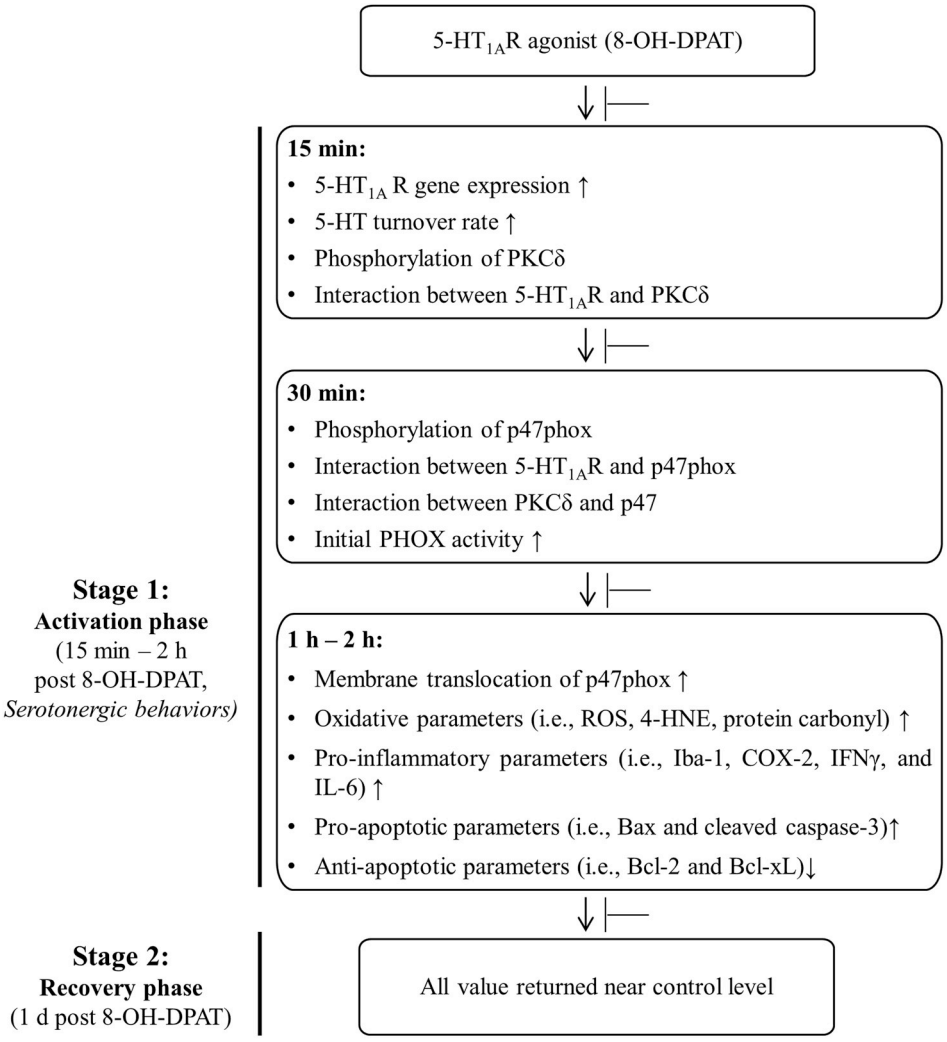

Fig. 14. A schematic depiction of the interaction between 5-HT_{1A}R and PKCδ/p47phox in 8-OH-DPAT-induced serotonergic behaviors in mice. Treatment with 8-OH-DPAT (2 mg/kg, i.p.) resulted in significant increases in the 5-HT_{1A} receptor gene expression and 5-HT turnover rate, followed by a significant phosphorylation of PKCδ in the hypothalamus of WT mice. PKCδ-dependent 5-HT_{1A}R activation occurred rapidly (15 min post-8-OH-DPAT). These initial cascades led to the activation of p47phox (30 min post 8-OH-DPAT), and resulted in PKCδ-dependent p47phox activation. Moreover, 8-OH-DPAT treatment resulted in the interaction between 5-HT_{1A}R and p47phox (30 min post-8-OH-DPAT). This phenomenon possibly contributes to serotonergic behaviors in mice. Thereafter, membrane translocation of p47phox, PHOX activity including oxidative parameters, and pro-inflammatory/pro-apoptotic changes occurred. Importantly, WAY100635 did not exhibit any additive effects against the attenuation offered by genetic inhibition of PKCδ or p47phox. 8-OH-DPAT-induced altered parameters (i.e., 5-HT turnover rate, 5-HT_{1A}R mRNA and protein expression, PKCδ phosphorylation, interaction between 5-HT_{1A}R and PKCδ, p47phox phosphorylation and p47phox membrane translocation, pro-inflammatory, and pro-apoptotic signalings) returned near control level within 24 h. Therefore, we propose that PKCδ initially mediates 8-OH-DPAT-induced serotonergic behaviors via 5-HT_{1A}R activation, and that inhibition of PKCδ-dependent p47phox activation (i.e., phosphorylation and membrane translocation) is critical for protecting against 8-OH-DPAT-induced serotonergic behaviors.

requires p47phox phosphorylation, which plays an important role in the translocation of cytosolic components to cytochrome *b*558, as well as in the assembly and activation of PHOX (Dang et al., 2006; El-Benna et al., 2008; Groemping and Rittinger, 2005; Qian et al., 2008). Therefore, it is plausible that phosphorylation of p47phox constitutes one of the key intracellular events associated with PHOX activation. We have shown that PHOX inhibitor apocynin prevents against methamphetamine insults via inhibition of extracellular signal-regulated kinases (ERK) 1/2-dependent of p47phox activation in mice (Dang et al., 2016). Thus, we raise the possibility that inhibition of PHOX/p47phox would be a possible therapeutic target for neuropsychotoxic disorders.

In addition, Reeves et al. (1999) reported that interaction occurs at the catalytic site of PKC and the C-terminus of p47phox, and is specific for p47phox (Reeves et al., 1999). Other earlier *in vitro* studies with phorbol 12-myristate 13-acetate (PMA)-stimulated neutrophils or B lymphocytes have also indicated that activation of PHOX requires phosphorylation of p47phox, which occurs prior to its translocation (DeLeo and Quinn, 1996; Johnson et al., 1998; Park and Ahn, 1995). Moreover, we recently suggested that PKCδ specifically regulates the function of PHOX in MA-induced neurotoxicty (Dang et al., 2018). Here we show that PKCδ co-immunoprecipitates with p47phox in the hypothalamus of mice, and that this interaction was inhibited by antagonism of 5-HT_{1A}R. Therefore, it is plausible that PKCδ is required for hypothalamic activation of PHOX by the phosphorylation and membrane translocation of p47phox.

It has been demonstrated that 5-HT alters the redox circumstances in a PHOX-dependent manner in Chinese hamster ovary (CHO) fibroblasts (Mukhin et al., 2000). Here we observed for the first time that 8-OH-DPAT significantly phosphorylates and translocates p47phox, and that 8-OH-DPAT induces oxidative burdens in the hypothalamus of mice, suggesting that 8-OH-DPAT-induced 5-HT release is via PHOX-dependent oxidative stress in the hypothalamus of mice. It was also demonstrated that the 5-HT is the main inducer of ROS in the hypothalamus (Fang et al., 2013). Therefore, we cannot rule out the possibility that the intracellular 5-HT-induced ROS formation might function directly via the 5-HT_{1A}R signaling pathway by PHOX.

In addition, it is possible that the functional regulation of PHOX activity by PKCδ is corroborated by our results showing that inhibition of PKCδ also blocks ROS formation, as well as serotonergic impairments. We also indicated that inhibition of PKCδ/p47phox or PKCδ-dependent p47phox activation provides significant protection against pro-apoptotic degeneration through a mechanism involving activation of Nrf2-dependent GSH induction (Dang et al., 2018). In addition, we reported that inhibition of PKCδ or p47phox markedly increased levels

of p-Akt, p-Bad, 14-3-3 protein-associated p-Bad, and Bcl-xL (Bcl-2), and decreased levels of Bax and cleaved caspase-3 (Dang et al., 2018).

In the line with our previous findings, we observed that 8-OH-DPAT treatment up-regulates pro-inflammatory parameters (i.e., Iba-1, COX-2, IFN-γ and IL-6) (Fig. 8), suggesting that activation of 5-HT_{1A}R leads to a pro-inflammation stage. However, because 8-OH-DPAT treatment did not significantly alter astrocytic parameter GFAP and TNF-α, this phenomenon remains to be further elucidated. In addition, 8-OH-DPAT also facilitated pro-apoptotic message by activating pro-apoptotic factors (i.e., Bax and cleaved caspase-3) and inhibiting anti-apoptotic factors (i.e., Bcl-2 and Bcl-xL) (Fig. 9). Consistently, it was demonstrated that 8-OH-DPAT promotes apoptosis in CHO cells by stimulating c-JUN N-terminal kinse-dependent pro-apoptotic pathways (Turner et al., 2007), and that 5-HT_{1A}R antagonist WAY100635 attenuates apoptosis induced by post-traumatic stress (Liu et al., 2011), suggesting that 5-HT_{1A}R activation facilitates pro-apoptosis. Therefore, our results suggest that neuroprotection by inhibition of PKCδ-dependent p47 phox activation is, at least in part, mediated by its anti-inflammatory/anti-apoptotic properties. However, precise molecular mechanism for the interaction between 5-HT_{1A}R and PKCδ/p47phox remains to be further elucidated.

In conclusion, our results suggest that 5-HT_{1A}R gene expression, p47phox activation, oxidants generation, and pro-inflammatory/pro-apoptotic changes via PKCδ activation are involved in 8-OH-DPAT-induced serotonergic behaviors. We also propose that interaction between the 5-HT_{1A}R/PKCδ and p47phox is critical for serotonergic behaviors induced by 8-OH-DPAT, and that the potential neuroprotective mechanism mediated by PKCδ/PHOX (p47phox) inhibition may provide a novel therapeutic intervention in response to serotonergic behaviors.

Conflicts of interest

The authors have no conflicts of interest to declare.

Acknowledgements

This study was supported by Basic Science Research Program through the National Research Foundation of Korea funded by the Ministry of Science and ICT (#NRF-2017R1A2B1003346 and #NRF-2016R1A1A1A05005201), Republic of Korea, and by a grant (17H04252) from the Japan Society for the Promotion of Science, Japan. Hai-Quyen Tran, Bao-Chau Hoai Nguyen, Dieu-Hien Phan, and Min-Ji Kang were supported by the BK21 PLUS program, National Research Foundation of Korea, Republic of Korea. The English in this document has been checked by at least two professional editors, both native speakers of English (Beverly Hills English; www.academiccommunications.com).

Appendix A. Supplementary data

Supplementary data to this article can be found online at https://doi.org/10.1016/j.fct.2018.10.049.

Transparency document

Transparency document related to this article can be found online at https://doi.org/10.1016/j.fct.2018.10.049.

References

Anji, A., Sullivan Hanley, N.R., Kumari, M., Hensler, J.G., 2001. The role of protein kinase C in the regulation of serotonin-2A receptor expression. J. Neurochem. 77, 589–597. https://doi.org/10.1046/j.1471-4159.2001.00261.x.

Babior, B.M., 1999. NADPH oxidase: an update. Blood 93, 1464–1476.

Bert, B., Fink, H., Hörtnagl, H., Veh, R.W., Davies, B., Theuring, F., Kusserow, H., 2006. Mice over-expressing the 5-HT1A receptor in cortex and dentate gyrus display exaggerated locomotor and hypothermic response to 8-OH-DPAT. Behav. Brain Res. 167, 328–341. https://doi.org/10.1016/j.bbr.2005.09.020.

Bijl, D., 2004. The serotonin syndrome. Neth. J. Med. 62, 309–313. https://doi.org/10.1056/NEJMra041867.

Billett, E.E., 2004. Monoamine oxidase (MAO) in human peripheral tissues. Neurotoxicology 25, 139–148. https://doi.org/10.1016/S0161-813X(03)00094-9.

Birmes, P., Coppin, D., Schmitt, L., Lauque, D., 2003. Serotonin syndrome: a brief review. Can. Med. Assoc. J. 168, 1439–1442.

Blanchard, R.J., Griebel, G., Guardiola-Lemaître, B., Brush, M.M., Lee, J., Blanchard, D.C., 1997. An ethopharmacological analysis of selective activation of 5-HT(1A) receptors: the mouse 5-HT(1A) syndrome. Pharmacol. Biochem. Behav. 57, 897–908. https://doi.org/10.1016/S0091-3057(96)00472-8.

Boyer, E.W., Shannon, M., 2005. The serotonin syndrome. N. Engl. J. Med. 35211352, 1112–1120. https://doi.org/10.1056/NEJMra041867.

Brown, T.M., Skop, B.P., Mareth, T.R., 1996. Pathophysiology and management of the serotonin syndrome. Ann. Pharmacother. 30, 527–533. https://doi.org/10.1177/106002809603000517.

Dang, D.K., Shin, E.J., Kim, D.J., Tran, H.Q., Jeong, J.H., Jang, C.G., Ottersen, O.P., Nah, S.Y., Hong, J.S., Nabeshima, T., Kim, H.C., 2018. PKCδ-dependent p47phox activation mediates methamphetamine-induced dopaminergic neurotoxicity. Free Radic. Biol. Med. 115, 318–337. https://doi.org/10.1016/j.freeradbiomed.2017.12.018.

Dang, D.K., Shin, E.J., Mai, A.T., Jang, C.G., Nah, S.Y., Jeong, J.H., Ledent, C., Yamamoto, T., Nabeshima, T., Onaivi, E.S., Kim, H.C., 2017a. Genetic or pharmacological depletion of cannabinoid CB1 receptor protects against dopaminergic neurotoxicity induced by methamphetamine in mice. Free Radic. Biol. Med. 108, 204–224. https://doi.org/10.1016/j.freeradbiomed.2017.03.033.

Dang, D.K., Shin, E.J., Nam, Y., Ryoo, S., Jeong, J.H., Jang, C.G., Nabeshima, T., Hong, J.S., Kim, H.C., 2016. Apocynin prevents mitochondrial burdens, microglial activation, and pro-apoptosis induced by a toxic dose of methamphetamine in the striatum of mice via inhibition of p47phox activation by ERK. J. Neuroinflammation 13, 12. https://doi.org/10.1186/s12974-016-0478-x.

Dang, D.K., Shin, E.J., Tran, H.Q., Kim, D.J., Jeong, J.H., Jang, C.-G., Nah, S.Y., Sato, H., Nabeshima, T., Yoneda, Y., Kim, H.C., 2017b. The role of system Xc(-) in methamphetamine-induced dopaminergic neurotoxicity in mice. Neurochem. Int. 108, 254–265. https://doi.org/10.1016/j.neuint.2017.04.013.

Dang, P.M.C., Stensballe, A., Boussetta, T., Raad, H., Dewas, C., Kroviarski, Y., Hayem, G., Jensen, O.N., Gougerot-Pocidalo, M.A., El-Benna, J., 2006. A specific p47phox-serine phosphorylated by convergent MAPKs mediates neutrophil NADPH oxidase priming at inflammatory sites. J. Clin. Invest. 116, 2033–2043. https://doi.org/10.1172/JCI27544.

DeLeo, F.R., Quinn, M.T., 1996. Assembly of the phagocyte NADPH oxidase: molecular interaction of oxidase proteins. J. Leukoc. Biol. 60, 677–691.

Domenicotti, C., Marengo, B., Verzola, D., Garibotto, G., Traverso, N., Patriarca, S., Maloberti, G., Cottalasso, D., Poli, G., Passalacqua, M., Melloni, E., Pronzato, M.A., Marinari, U.M., 2003. Role of PKCδ activity in glutathione-depleted neuroblastoma cells. Free Radic. Biol. Med. 35, 504–516. https://doi.org/10.1016/S0891-5849(03)00332-0.

El-Benna, J., Dang, P.M.C., Gougerot-Pocidalo, M.A., 2008. Priming of the neutrophil NADPH oxidase activation: role of p47phox phosphorylation and NOX2 mobilization to the plasma membrane. Semin. Immunopathol. 30, 279–289. https://doi.org/10.1007/s00281-008-0118-3.

Fang, X.L., Shu, G., Yu, J.J., Wang, L.N., Yang, J., Zeng, Q.J., Cheng, X., Zhang, Z.Q., Wang, S.B., Gao, P., Zhu, X.T., Xi, Q.Y., Zhang, Y.L., Jiang, Q.Y., 2013. The anorexigenic effect of serotonin is mediated by the generation of NADPH oxidase-dependent ROS. PloS One 8, 1–8. https://doi.org/10.1371/journal.pone.0053142.

Fox, M.A., Jensen, C.L., Gallagher, P.S., Murphy, D.L., 2007. Receptor mediation of exaggerated responses to serotonin-enhancing drugs in serotonin transporter (SERT)-deficient mice. Neuropharmacology 53, 643–656. https://doi.org/10.1016/j.neuropharm.2007.07.009.

Gillman, K., 2004. Moclobemide and the risk of serotonin toxicity (or serotonin syndrome). CNS Drug Rev. 10, 83–85. author reply 86-8. https://doi.org/10.1111/j.1527-3458.2004.tb00005.x.

Giorgi, C., Agnoletto, C., Baldini, C., Bononi, A., Bonora, M., Marchi, S., Missiroli, S., Patergnani, S., Poletti, F., Rimessi, A., Zavan, B., Pinton, P., 2010. Redox control of protein kinase C: cell-and disease-specific aspects. Antioxidants Redox Signal. 13, 1051–1085. https://doi.org/10.1089/ars.2009.2825.

Gopalakrishna, R., Jaken, S., 2000. Protein kinase C signaling and oxidative stress. Free Radic. Biol. Med. 28, 1349–1361. https://doi.org/16/S0891-5849(00)00221-5.

Graudins, A., Stearman, A., Chan, B., 1998. Treatment of the serotonin syndrome with cyproheptadine. J. Emerg. Med. 16, 615–619. https://doi.org/https://doi.org/10.1016/S0736-4679(98)00057-2.

Groemping, Y., Rittinger, K., 2005. Activation and assembly of the NADPH oxidase: a structural perspective. Biochem. J. 386, 401–416. https://doi.org/10.1042/BJ20041835.

Haberzettl, R., Bert, B., Fink, H., Fox, M.A., 2013. Animal models of the serotonin syndrome: a systematic review. Behav. Brain Res. 256, 328–345. https://doi.org/10.1016/j.bbr.2013.08.045.

Haberzettl, R., Fink, H., Bert, B., 2014. Role of 5-HT1A- and 5-HT2Areceptors for the murine model of the serotonin syndrome. J. Pharmacol. Toxicol. Methods 70, 129–133. https://doi.org/10.1016/j.vascn.2014.07.003.

Isbister, G.K., Bowe, S.J., Dawson, A., Whyte, I.M., 2004. Relative toxicity of selective serotonin reuptake inhibitors (SSRIs) in overdose. J. Toxicol. Clin. Toxicol. 42, 277–285.

Izumi, T., Iwamoto, N., Kitaichi, Y., Kato, A., Inoue, T., Koyama, T., 2006. Effects of co-administration of a selective serotonin reuptake inhibitor and monoamine oxidase inhibitors on 5-HT-related behavior in rats. Eur. J. Pharmacol. 532, 258–264. https://doi.org/10.1016/j.ejphar.2005.12.075.

Jacobs, B.L., 1976. An animal behavior model for studying central serotonergic synapses. Life Sci. 19, 777–785. https://doi.org/10.1016/0024-3205(76)90303-9.
Johnson, J.L., Park, J., Benna, J. El, Faust, L.P., Inanami, O., Babior, B.M., 1998. Activation of p47 PHOX. a Cytosolic Subunit of the Leukocyte 273, 35147–35152.
Kalueff, A.V., LaPorte, J.L., Murphy, D.L., 2008. Perspectives on genetic animal models of serotonin toxicity. Neurochem. Int. 52, 649–658. https://doi.org/10.1016/j.neuint.2007.08.015.
Kaneda, Y., Ohmori, T., Okabe, H., 2001. Possible mild serotonin syndrome related to co-prescription of tandospirone and trazodone. Gen. Hosp. Psychiatr. 23 (2), 98–101.
Liu, W., Chen, Q., Liu, J., Liu, K.J., 2011. Normobaric hyperoxia protects the blood brain barrier through inhibiting Nox2 containing NADPH oxidase in ischemic stroke. Med. Gas Res. 1, 22. https://doi.org/10.1186/2045-9912-1-22.
Liu, Y.F., Albert, P.R., 1991. Cell-specific signaling of the 5-HT1A receptor. Modulation by protein kinases C and A. J. Biol. Chem. 266, 23689–23697.
Middleton, J.P., Albers, F.J., Dennis, V.W., Raymond, J.R., 1990. Thapsigargin demonstrates calcium-dependent regulation of phosphate uptake in HeLa cells. Am. J. Physiol. Renal. Physiol. 259 F727 LP-F731.
Miyamoto, A., Nakayama, K., Imaki, H., Hirose, S., Jiang, Y., Abe, M., Tsukiyama, T., Nagahama, H., Ohno, S., Hatakeyama, S., Nakayama, K.I., 2002. Increased proliferation of B cells and auto-immunity in mice lacking protein kinase Cδ. Nature 416, 865–869. https://doi.org/10.1038/416865a.
Mukhin, Y.V., Garnovskaya, M.N., Collinsworth, G., GrewalL, J.S., Pendergrass, D., Nagai, T., Pinckney, S., Greene, E.L., Raymond, J.R., 2000. 5-Hydroxytryptamine1A receptor/Giβγ stimulates mitogen-activated protein kinase via NAD(P)H oxidase and reactive oxygen species upstream of Src in Chinese hamster ovary fibroblasts. Biochem. J. 347 61 LP-67.
Nguyen, X.K.T., Lee, J., Shin, E.J., Dang, D.K., Jeong, J.H., Nguyen, T.T.L., Nam, Y., Cho, H.J., Lee, J.C., Park, D.H., Jang, C.G., Hong, J.S., Nabeshima, T., Kim, H.C., 2015. Liposomal melatonin rescues methamphetamine-elicited mitochondrial burdens, pro-apoptosis, and dopaminergic degeneration through the inhibition PKCδ gene. J. Pineal Res. 58, 86–106. https://doi.org/10.1111/jpi.12195.
Nisijima, K., 2000. Abnormal monoamine metabolism in cerebrospinal fluid in a case of serotonin syndrome. J. Clin. Psychopharmacol.
Nisijima, K., Yoshino, T., Ishiguro, T., 2000. Risperidone counteracts lethality in an animal model of the serotonin syndrome. Psychopharmacology 150, 9–14.
Nitti, M., D'Abramo, C., Traverso, N., Verzola, D., Garibotto, G., Poggi, A., Odetti, P., Cottalasso, D., Marinari, U.M., Pronzato, M.A., Domenicotti, C., 2005. Central role of PKCδ in glycoxidation-dependent apoptosis of human neurons. Free Radic. Biol. Med. 38, 846–856. https://doi.org/10.1016/j.freeradbiomed.2004.12.002.
Oliver, C.N., Ahn, B.W., Moerman, E.J., Goldstein, S., Stadtman, E.R., 1987. Age-related changes in oxidized proteins. J. Biol. Chem. 262, 5488–5491.
Park, J.W., Ahn, S.M., 1995. Translocation of recombinant p47phox cytosolic component of the phagocyte oxidase by in vitro phosphorylation. Biochem. Biophys. Res. Commun. 211, 410–416. https://doi.org/10.1006/bbrc.1995.1829.
Qian, L., Wei, S.J., Zhang, D., Hu, X., Xu, Z., Wilson, B., El-Benna, J., Hong, J.S., Flood, P.M., 2008. Potent anti-inflammatory and neuroprotective effects of TGFβ1 are mediated through the inhibition of ERK and p47phox-ser345 phosphorylation and translocation in microglia. J. Immunol. 181, 660–668. https://doi.org/10.4049/jimmunol.181.1.660.
Ramamoorthy, S., Giovanetti, E., Qian, Y., Blakely, R.D., 1998. Phosphorylation and Regulation of Antidepressant-sensitive Serotonin Transporters *, vol. 273. pp. 2458–2466.
Raymond, J.R., Fargin, A., Middleton, J.P., Graff, J.M., Haupt, D.M., Caron, M.G., Lefkowitz, R.J., Dennis, V.W., 1989. The human 5-HT1A receptor expressed in HeLa cells stimulates sodium-dependent phosphate uptake via protein kinase C. J. Biol. Chem. 264, 21943–21950.
Raymond, J.R., Mukhin, Y.V., Gelasco, a, Turner, J., Collinsworth, G., Gettys, T.W., Grewal, J.S., Garnovskaya, M.N., 2001. Multiplicity of mechanisms of serotonin receptor signal transduction. Pharmacol. Ther. 92, 179–212. https://doi.org/10.1016/S0163-7258(01)00169-3.
Reeves, E.P., Dekker, L.V., Forbes, L.V., Wientjes, F.B., Grogan, A., Pappin, D.J.C., Segal, A.W., 1999. Direct interaction between p47phox and protein kinase C: evidence for targeting of protein kinase C by p47phox in neutrophils. Biochem. J. 334, 859–866. https://doi.org/10.1042/0264-6021:3440859.
Shimomura, K., Mori, J., Honda, F., 1981. Backward walking induced by L-5-hydroxytryptophan in mice. Jpn. J. Pharmacol. 31, 39–46.
Shin, E.J., Duong, C.X., Nguyen, X.K.T., Bing, G., Bach, J.H., Park, D.H., Nakayama, K., Ali, S.F., Kanthasamy, A.G., Cadet, J.L., Nabeshima, T., Kim, H.C., 2011. PKCdelta inhibition enhances tyrosine hydroxylase phosphorylation in mice after methamphetamine treatment. Neurochem. Int. 59, 39–50. https://doi.org/10.1016/j.neuint.2011.03.022.
Shin, E.J., Duong, C.X., Nguyen, X.K.T., Li, Z., Bing, G., Bach, J.H., Park, D.H., Nakayama, K., Ali, S.F., Kanthasamy, A.G., Cadet, J.L., Nabeshima, T., Kim, H.C., 2012. Role of oxidative stress in methamphetamine-induced dopaminergic toxicity mediated by protein kinase Cdelta. Behav. Brain Res. 232, 98–113. https://doi.org/10.1016/j.bbr.2012.04.001.
Shin, E.J., Nam, Y., Tu, T.H.T., Lim, Y.K., Wie, M.B., Kim, D.J., Jeong, J.H., Kim, H.C., 2016. Protein kinase Cdelta mediates trimethyltin-induced neurotoxicity in mice in vivo via inhibition of glutathione defense mechanism. Arch. Toxicol. 90, 937–953. https://doi.org/10.1007/s00204-015-1516-7.
Shin, E.J., Shin, S.W., Nguyen, T.T.L., Park, D.H., Wie, M.B., Jang, C.G., Nah, S.Y., Yang, B.W., Ko, S.K., Nabeshima, T., Kim, H.C., 2014. Ginsenoside Re rescues methamphetamine-induced oxidative damage, mitochondrial dysfunction, microglial activation, and dopaminergic degeneration by inhibiting the protein kinase Cδ gene. Mol. Neurobiol. 49, 1400–1421. https://doi.org/10.1007/s12035-013-8617-1.
Shioda, K., Nisijima, K., Yoshino, T., Kato, S., 2004. Extracellular serotonin, dopamine and glutamate levels are elevated in the hypothalamus in a serotonin syndrome animal model induced by tranylcypromine and fluoxetine. Prog. Neuro-Psychopharmacol. Biol. Psychiatry 28, 633–640. https://doi.org/10.1016/j.pnpbp.2004.01.013.
Sloviter, R.S., Drust, E.G., Connor, J.D., 1978. Specificity of a rat behavioral model for serotonin receptor activation. J. Pharmacol. Exp. Therapeut. 206 339 LP-347.
Smith, L.M., Peroutka, S.J., 1986. Differential effects of 5-hydroxytryptamine1a selective drugs on the 5-HT behavioral syndrome. Pharmacol. Biochem. Behav. 24, 1513–1519.
Sorce, S., Stocker, R., Seredenina, T., Holmdahl, R., Aguzzi, A., Chio, A., Depaulis, A., Heitz, F., Olofsson, P., Olsson, T., Duveau, V., Sanoudou, D., Skosgater, S., Vlahou, A., Wasquel, D., Krause, K.H., Jaquet, V., 2017. NADPH oxidases as drug targets and biomarkers in neurodegenerative diseases: what is the evidence? Free Radic. Biol. Med. 112, 387–396. https://doi.org/10.1016/j.freeradbiomed.2017.08.006.
Squires, L.N., Jakubowski, J.A., Stuart, J.N., Rubakhin, S.S., Hatcher, N.G., Kim, W.S., Chen, K., Shih, J.C., Seif, I., Sweedler, J.V., 2006. Serotonin catabolism and the formation and fate of 5-hydroxyindole thiazolidine carboxylic acid. J. Biol. Chem. 281, 13463–13470. https://doi.org/10.1074/jbc.M602210200.
Thanacoody, R., 2012. Serotonin syndrome. Medicine (Baltim.) 40, 63–64. https://doi.org/10.1016/j.mpmed.2011.11.005.
Tran, H.Q., Lee, Y., Shin, E.J., Jang, C.G., Jeong, J.H., Mouri, A., Saito, K., Nabeshima, T., Kim, H.C., 2018. PKCδ knockout mice are protected from dextromethorphan-induced serotonergic behaviors in mice: involvements of downregulation of 5-HT1A receptor and upregulation of Nrf2-dependent GSH synthesis. Mol. Neurobiol. 55, 7802–7821. https://doi.org/10.1007/s12035-018-0938-7.
Tran, T.V., Shin, E.J., Jeong, J.H., Lee, J.W., Lee, Y., Jang, C.G., Nah, S.Y., Lei, X.G., Toriumi, K., Yamada, K., Nabeshima, T., Kim, H.C., 2017. Protective potential of the glutathione peroxidase-1 gene in abnormal behaviors induced by phencyclidine in mice. Mol. Neurobiol. 54, 7042–7062. https://doi.org/10.1007/s12035-016-0239-y.
Turner, J.H., Garnovskaya, M.N., Raymond, J.R., 2007. Serotonin 5-HT1Areceptor stimulates c-Jun N-terminal kinase and induces apoptosis in Chinese hamster ovary fibroblasts. Biochim. Biophys. Acta Mol. Cell Res. 1773, 391–399. https://doi.org/10.1016/j.bbamcr.2006.12.003.
Wang, Q., Shin, E.J., Nguyen, X.K.T., Li, Q., Bach, J.H., Bing, G., Kim, W.K., Kim, H.C., Hong, J.S., 2012. Endogenous dynorphin protects against neurotoxin-elicited nigrostriatal dopaminergic neuron damage and motor deficits in mice. J. Neuroinflammation 9, 583. https://doi.org/10.1186/1742-2094-9-124.
Watts, S.W., Morrison, S.F., Davis, R.P., Barman, S.M., 2012. Serotonin and blood pressure regulation. Pharmacol. Rev. 64, 359–388. https://doi.org/10.1124/pr.111.004697.
Yamada, J., Sugimoto, Y., Horisaka, K., 1988. The behavioural effects of 8-hydroxy-2-(di-n-propylamino)tetralin (8-OH-DPAT) in mice. Eur. J. Pharmacol. 154, 299–304.
Yu, H., Lewander, T., 1997. Pharmacokinetic and pharmacodynamic studies of (R)-8-hydroxy-2-(di-n-propylamino)tetralin in the rat. Eur. Neuropsychopharmacol 7, 165–172.
Zhang, D., Hu, X., Wei, S.-J., Liu, J., Gao, H., Qian, L., Wilson, B., Liu, G., Hong, J.-S., 2008. Squamosamide derivative FLZ protects dopaminergic neurons against inflammation-mediated neurodegeneration through the inhibition of NADPH oxidase activity. J. Neuroinflammation 5, 21. https://doi.org/10.1186/1742-2094-5-21.